



Soil nickel contamination levels entail changes in the bacterial communities associated to the rhizosphere and endosphere of *Odontarrhena chalcidica*

Alexis Durand · Xavier Goux · Séverine Lopez ·
Pierre Leglize · Emile Benizri 

Received: 7 March 2023 / Accepted: 2 August 2023 / Published online: 11 August 2023
© The Author(s), under exclusive licence to Springer Nature Switzerland AG 2023

Abstract

Aims Phytomining relies on the use of metal hyper-accumulating plants growing on ultramafic soils. Such soils, naturally enriched with nickel, have drawn the attention of the scientific community for several decades, yet little is known about the effect of this metal on the structure and composition of the rhizosphere and endospheric bacterial communities of hyperaccumulators. This work aimed to investigate the impact of a Ni concentration gradient on soil's physicochemical properties and on the composition of the rhizosphere and endophytic bacterial communities of *Odontarrhena chalcidica*.

Methods We characterized the bacterial communities associated with *O. chalcidica* growing in controlled conditions on an ultramafic soil with various

levels of nickel contamination obtained by spiking the soil with nickel sulfate.

Results An increase in the available nickel in soil induced changes in the dominant bacterial genera in the communities of the rhizosphere soil and in the root and shoot endosphere. This increase in available nickel also entailed changes in the relative abundance of the predicted functions, for the rhizosphere and root endospheric bacterial communities. In addition, topological features of the bacterial networks seemed to indicate that at an intermediate level of nickel contamination, two coexisting bacterial sub-communities were in competition, one adapted to “low” soil nickel content and the other to higher nickel content, while the bacterial communities were more stable at the lowest and the highest nickel soil contamination levels. Our results revealed shifts in the microbial community's structure and functions, depending of the gradient of soil nickel availability in the soil.

Responsible Editor: Juan Barcelo.

Supplementary Information The online version contains supplementary material available at <https://doi.org/10.1007/s11104-023-06215-z>.

A. Durand · P. Leglize · E. Benizri (✉)
Université de Lorraine, INRAE, LSE, F-54000 Nancy,
France
e-mail: emile.benizri@univ-lorraine.fr

X. Goux
Microbiome Engineering Group, Luxembourg Institute
of Science and Technology, 4422 Belvaux, Luxembourg

S. Lopez
INRAE, SAVE, F-33882 Villenave d'Ornon, France

Keywords Bacterial diversity · Hyperaccumulator · Nickel · Soil microbial community · Endophyte · High-throughput sequencing

Introduction

Ultramafic soils (*i.e.* serpentine soils) are atypical soils that derive from ultramafic rocks composed of ferromagnesian silicates and are known to contain significant concentrations of nickel (Ni) ranging

between 1.0 and 7.0 g kg⁻¹ (Chaney et al. 2008). They are found worldwide, but with a patchy distribution, covering ~3% of the terrestrial surface (Echevarria 2018) with more than 400,000 ha in California and Oregon (Alexander 1994), 100,000 ha in Albania (Bani et al. 2018), and 150,000 ha in Indonesia (van der Ent et al. 2013). These soils present geochemical peculiarities, which include an elevated concentration of magnesium (Mg) and iron (Fe). They are also known for their deficiency in macronutrients and present a poor availability of essential plant nutrients including nitrogen (N), phosphorus (P), potassium (K) and calcium (Ca) (Boyd and Jaffré 2009; Nkrumah et al. 2016; Saad et al. 2018).

The low-fertility and low-productivity of ultramafic soils make them unattractive for traditional agriculture and many of these lands are slowly abandoned by farmers, with rural exodus (Saad et al. 2016). However, these ultramafic landscapes have potential to provide multiple ecosystem services and contribute to Europe's goals towards insuring production of renewable raw materials and renewable energy (Echevarria et al. 2015). The idea of phytomining metals emerged in the 90 s (Chaney et al. 2008; Bani et al. 2015; van der Ent et al. 2015) with the objective of extracting metal trace elements from metal-rich soil using hyperaccumulator plant, that are capable of absorbing and transferring these elements to their aerial parts where they are accumulated (Chaney et al. 2007). Then, the aerial parts (*i.e.*, shoots) are incinerated to ash to obtain a “bio-ore”, with high concentrations of target metals, such as Ni and it is possible to recycle metals for industrial use (Barbaroux et al. 2011), underlying that this technology can be considered as a commercially viable technique in the case of high-value elements such as Ni, Co, or Au (Chaney et al. 2018). In fact, when growing in such metal-enriched substrates, hyperaccumulators can accumulate metals in their living tissues up to hundreds or often thousands times more than “normal” plants (Reeves 2003; van der Ent et al. 2015). *Odon-tarrhena chalcidica* (Janka) (Španiel et al. 2015) (previous name *Alyssum murale* Waldst & Kit.) is a Ni-hyperaccumulating plant that has received a lot of attention due to its extraordinary ability to extract Ni from soils and accumulate it in its tissues. This plant is common in ultramafic zones from the Eastern Mediterranean, and able to accumulate Ni to concentrations exceeding 2% of its dry weight (Bani et al.

2015). Its biomass containing 20 000 µg g⁻¹ Ni translates to 32 wt% Ni in the ash (Li et al. 2003; Corzo Remigio et al. 2020).

Phytoextraction of metals has benefited from work on the role of rhizosphere microorganisms. Indeed, several researches reported the potential of remediation of soil contaminated by heavy metals using hyperaccumulating plants associated with plant growth promoting rhizobacteria (PGPR) (Zhuang et al. 2007; Lebeau et al. 2008; Ma et al. 2009b; Glick 2010; Sessitsch et al. 2013; Cabello-Conejo et al. 2014; Durand et al. 2016). Among these microorganisms, some increase the plant biomass (Rajkumar and Freitas 2008; Kumar et al. 2008, 2009; Ma et al. 2009a; Cabello-Conejo et al. 2014; Durand et al. 2016) *via* the production of hormone-like molecules. Others also promote the resistance of plants to the stress exerted by the metal *via* the production of 1-aminocyclopropane-1-carboxylate (ACC) deaminase, with a consequent decrease in the synthesis of ethylene in plant tissues. These effects resulted in a better plant development (Cabello-Conejo et al. 2014; Glick 2010, 2005; Lebeau et al. 2008; Ma et al. 2011b) and lead to an improvement of metal uptake and hyperaccumulation (Abou-Shanab et al. 2003; Rajkumar et al. 2012; Visioli et al. 2015). Recently, many endophytes have been found to be resistant to heavy metals and endophyte-assisted phytoremediation has been highly recommended as a promising technology for *in situ* remediation of contaminated soils. Plant growth promoting endophytic bacteria (PGPE) are considered as a subclass PGPR (Reinhold-Hurek and Hurek 1998; Afzal et al. 2019). They share all the important traits consistent with the host plant growth promotion found in rhizobacteria. Indeed, these bacteria can benefit host plants by improving plant nutrition or by producing phytohormones that modulate plant growth and stress. Moreover they can improve plant health, reducing pathogen attacks with antibiotics, and hydrolytic enzymes (Durand et al. 2021). Other beneficial plant physiological changes have been observed following bacterial endophyte inoculations, including accumulation of osmolytes, osmotic adjustment, stomatal regulation, reduced membrane potentials, as well as changes in phospholipid content in the cell membranes (Compant et al. 2005; Ma et al. 2011a). However, the beneficial effects provided by the endophytic bacteria to host plants are usually greater than those provided by many rhizosphere bacteria (Pillay

and Nowak 2011; Afzal et al. 2019) and especially when plants are growing under either biotic or abiotic stress conditions (Ait Barka et al. 2006). It is therefore clear why phytoremediation assisted by endophytic bacteria has been strongly recommended, given that their beneficial effects may be exacerbated when plants are challenged by stress conditions such as soil metal pollutions (Hardoim et al. 2008) and thereby lead to better metal uptake and translocation, as well as to an increase in the metal bioavailability (Sessitsch et al. 2013; Ma et al. 2016).

There are numerous reports of hyperaccumulating plant growth promotion by endophytic bacteria (Idris and Trifonova 2004; Barzanti et al. 2007; Ma et al. 2011a). Many of these studies have focused on promoting plant growth under environmental stress, such as soil metal pollution. However, only a few of them have attempted to explore the endophytic bacterial community diversity associated with these hyperaccumulating plants (Lu et al. 2013; Su et al. 2016) and even fewer to describe the responses of such communities to increased levels of stress, such as the presence of metal in soil. Indeed, information relevant to the impacts of pollutants on the endophytic bacterial community of hyperaccumulating plants is scarce.

To date, it is unclear whether the level of soil metal concentration influences microbial communities in the rhizosphere and the endosphere of a nickel hyperaccumulator. However, in order to improve the phytoremediation efficiency of hyperaccumulating plants, it is important to address this question. In this study, a gradient of Ni concentration in an ultramafic soil was used to investigate its impact on the soil physicochemical properties as well as on the rhizosphere and endophytic bacterial communities associated with *O. chalcidica*. This study will provide information regarding the phytomining potential of *O. chalcidica* and improve our understanding of interactions among soil-Ni-plant systems and rhizosphere and endophytic bacterial communities.

Materials and methods

Experimental design

A pot experiment, using the hyperaccumulating plant *Odontarrhena chalcidica* (syn. *Alyssum murale*, (Španiel et al. 2015)) was conducted for 7 months

in a growth chamber. *O. chalcidica* seeds were harvested from a natural site near Trigona (39°47'17.5" N, 21°25'19.1" E, Greece) in August 2014. The soil used for the experiment was collected from the topsoil of the region of Melide (Spain, 42°49'54.5" N, 8°00'13.5" W, Agolada, Pontevedra) and corresponded to an ultramafic soil. Soil physicochemical properties were determined by the Soil Analysis Laboratory of INRAE (Arras, France). This topsoil contained 14.5% clay, 32.3% silt and 52.6% sand, had a C/N ratio of 14.2, a Mg/Ca ratio of 1.37 and an available phosphorus content (P-Olsen) of 7 mg kg⁻¹. Soil pH was 5.25 and the total and diethylenetriamine pentaacetic acid (DTPA) extractable Ni (Ni-DTPA) contents were 850.1 and 18.9 mg Ni kg⁻¹ of dry soil, respectively. This soil was sieved to < 5 mm to remove coarse fragments and then artificially enriched with Ni sulfate (NiSO₄·7H₂O) with three different increasing concentrations (treatment D0, D1 and D2) corresponding to the following contamination levels: D0 (control)—natural content, D1: natural content plus 20 mg Ni kg⁻¹ of dry soil, D2: natural content plus 80 mg Ni kg⁻¹ of dry soil. For each treatment, four replicates were performed.

Pots were placed in a growth-chamber, with a randomized block design, under controlled conditions (photoperiod 16-h, day/night temperature 23 °C/19 °C, relative humidity level 80% and photosynthetic photon flux density 350 μmol m⁻² s⁻¹). The pots used were cylindrical (15 cm in diameter and 17 cm deep) and were filled with 1407 g of dry soil. Before sowing the seeds, the soil was incubated for three weeks. After this period, seeds were sown in each pot and the pots were watered with distilled water three times a week to 60% of soil water holding capacity, for 190 days after sowing, then to 50% until the harvest. Two months after sowing, the Mg/Ca ratio was improved and the N, P and K contents were adjusted by amending the soil with 300 mg kg⁻¹ of dry soil of CaSO₄, 152.52 mg kg⁻¹ of dry soil of KH₂PO₄ and 60 kg ha⁻¹ of CH₄NO₃.

Sample collection

Fresh root and shoot tissue samples were collected in 50 ml tubes at the harvest (211 days after sowing). In order to sterilize the outer surface, the plant parts were immersed and agitated in 30 mL of a 1% HClO solution supplemented with 0.1% Triton X100

for 30 s. Then, the plant parts were immersed in 95% ethanol for 30 s. Subsequently, they were rinsed five times with sterile distilled water. Plant parts (roots and shoots) and soil were conserved at $-80\text{ }^{\circ}\text{C}$. Plant part sterilization was confirmed by PCR, using the final rinsing water as a sample (Sánchez-López et al. 2018). PCR was designed to target the bacterial 16S rRNA gene using the following primers: 27f (5'-AGA GTT TGA TCA TGG CTC A -3') and 1492r (5'-TAC GGT TAC CTT GTT ACG ACT T -3') (Eurofins Genomics, Paris, France), and using the thermoscientific DreamTaq™ Green PCR Master Mix (2X) kit (Thermo Fisher Scientific, Carlsbad, California). For each PCR mix, 12.5 μL of Dream Taq Green master mix were used, each universal primer was adjusted to 0.4 μM , 2 μL of the final rinsing water were added and the final volume was adjusted to 25 μL with nuclease-free water. DNA amplification was carried out in a thermocycler (Mastercycler gradient, Eppendorf, Hamburg, Germany) under the following conditions: $95\text{ }^{\circ}\text{C}$ 2 min, 30 cycles $95\text{ }^{\circ}\text{C}$ 30 s, $53\text{ }^{\circ}\text{C}$ 30 s, and $72\text{ }^{\circ}\text{C}$ 1 min, with an additional 10 min at $72\text{ }^{\circ}\text{C}$. As positive control, 2 μL of bacterial DNA from isolated strain adjusted to $10\text{ ng }\mu\text{L}^{-1}$ was used.

Fresh rhizosphere soil was sampled by taking soil adhering to roots. Samples were kept at $4\text{ }^{\circ}\text{C}$ before microbial analyses. Two grams of fresh rhizosphere soil were frozen at $-80\text{ }^{\circ}\text{C}$ for further molecular analyses. A part of the rhizosphere soil set aside for the physicochemical analyses, was dried at $40\text{ }^{\circ}\text{C}$ in an oven.

Plant analyses

Elemental analyses were performed on subsamples (0.5 g) of dry and ground plant tissue after an acid-digestion with 2.5 ml of concentrated HNO_3 (14.65 M) and 5 mL of H_2O_2 (30%) at $95\text{ }^{\circ}\text{C}$. The final solutions were filtered (0.45 μm DigiFILTER, SCP Science, Canada) and topped up to 25 mL with deionized water. An Inductively Coupled Plasma-Atomic Emission Spectrometer (ICP-AES, Liberty II, Varian) was used to measure the elemental concentrations. The total C and N in the plant tissue were analyzed by combustion at $900\text{ }^{\circ}\text{C}$ with a CHNS analyzer (vario MICRO cube, Elementar Analysensysteme GmbH). A bioconcentration factor (BCF) was employed to quantify Ni-accumulation efficiency in plants, by comparing the concentration in the plant

parts (roots and aerial plant parts) and in the external medium (Ni concentration in soil at the beginning of the experiment), using the following formula: $\text{BCF} = \text{C}_p/\text{C}_s$, where C_p and C_s are Ni concentrations in plant parts (mg kg^{-1}) and pseudo-total concentration of Ni in soil, respectively (Zayed et al. 1998). Ni-translocation from root to shoot in plants was calculated using the following formula: $\text{TF} = \text{C}_s/\text{C}_r$, where TF was a translocation factor, and C_s and C_r were Ni concentrations (mg kg^{-1}) in the shoot and root, respectively (Tappero et al. 2007).

Soil physicochemical analyses

Soil samples were dried ($105\text{ }^{\circ}\text{C}$) until a constant weight was reached in order to determine soil moisture. Subsamples (0.5 g) of dry soil were acid-digested in 2 mL of concentrated HNO_3 and 6 mL of concentrated HCl for the quantification of major and trace elements, after being further analyzed with an ICP-AES. The available elements in the soil samples were extracted with a DTPA-TEA solution (0.005 M DTPA, 0.01 M CaCl_2 , 0.1 M triethanolamine, pH 7.3) (Lindsay and Norvell 1978) and the elements concentrations in solutions were measured with an ICP-AES. DTPA extraction was chosen, as DTPA is normalized as a soil analysis for the characterization of the availability of micro-nutrient in soils (such as Cu, Zn, Fe, and Mn) and it accesses the exact pool of isotopically-exchangeable Ni (Echevarria et al. 2006). Moreover, it is a recommended method (International Standard NF ISO 14870) for quantifying the labile/available pool (Kierczak et al. 2021). Soil pH was measured using a pH meter in a soil-water suspension (soil:water ratio = 1:5, v:v). Total and organic C and N were quantified with a CHNS analyzer.

Soil microbial analyses

Quantifications of microbial biomass carbon (MBC) and nitrogen (MBN) were performed on fresh rhizosphere soils. These microbial biomasses were determined by chloroform fumigation of 10 g of fresh soil for 24 h at $25\text{ }^{\circ}\text{C}$. Fumigated and non-fumigated soil samples were then extracted by agitation in 40 mL of K_2SO_4 (0.5 M) for 45 min and at 17 rpm. Solutions were filtered (Whatman 42), before being analyzed by a TOC analyzer. Calculations were made with a conversion coefficient K of 0.45 and 0.54 for MBC and

MBN, respectively (Brookes et al. 1985). Fluorescein diacetate activity (FDA) was measured according to the method described by Adam and Duncan (2001).

DNA extraction, amplification, and sequencing

At harvest, genomic DNA was extracted from soil samples using the FastDNA™ SPIN kit for Soil (MP Biomedicals™, France) in accordance with the manufacturer's protocol. Sterile plant parts (roots and shoots) were lyophilized and then ground in sterile conditions, into a homogenous powder with a Mixer Mill for 30 s at 30 Hz (model MM400; Retsch Inc., Newtown, Pennsylvania, 158 USA) and 5 mm zirconium oxide beads. DNA was extracted using a modified hexadecyltrimethylammonium bromide (CTAB) chloroform protocol (Healey et al. 2014). To recover enough DNA, each sample was mixed for 1 h at 65 °C with multiple agitation in the CTAB buffer (2 g CTAB, 4 mL EDTA 0,5 M, 10 ml TrisHCl 1 M and 86 mL NaCl 1,4 M in 100 mL), before undergoing a heat shock (-80 °C to 65 °C) and enzymatic digestions with proteinase K, α -amylase from *Aspergillus oryzae* and RNase A. The DNA precipitation was obtained firstly with isopropanol (at ambient temperature) and next with ethanol 70% (at 4 °C). A purification step was added using the QIAquick® PCR Purification Kit (Qiagen, Germany). The quantity and quality of purified DNA were assessed using electrophoresis migration on a 1% agarose gel and with a SmartSpec™ Plus spectrophotometer (BIO-RAD, made in USA). The PCR targeted the V5-V6 hypervariable regions of the bacterial 16S rRNA gene with chloroplast DNA excluding primers 799f (5'- AAC MGG ATT AGA TAC CCK G -3') and 1115r (5'- AGG GTT GCG CTC GTT G -3') resulting in an amplicon of small size (~316 bp) appropriate for Illumina sequencing (Kembel et al. 2014). Primers were modified with a 5' tail that added a barcode and an Illumina adaptor sequence following partner recommendations (Luxembourg Institute of Science and Technology, Luxembourg). The PCR reaction was achieved in triplicate, in equimolar concentrations, for each sample according to the following thermal profile: 3 min at 94 °C followed by 35 cycles at 94 °C for 45 s, 30 s at 56 °C, 90 s at 72 °C, and finally 10 min at 72 °C. After pooling the triplicate PCR products, these were further bead-purified (Agencourt

AMPure XP, Beckman Coulter) and the concentration was assessed with Qubit dsDNA HS Assay Kit. One ng of each purified product was used in a second round of PCR, together with 5 μ L of each of the index primers (Nextera XT Index Kit V2 Set C, Illumina) per sample. Reaction conditions of the second PCR were as follows: 98 °C for 30 s, followed by 8 cycles at 98 °C for 5 s, at 55 °C for 30 s and 72 °C for 30 s, and a final extension at 72 °C for 2 min. Purified libraries were pooled in equimolar ratios and this pool was assessed by quantitative polymerase chain reaction (qPCR), using KAPA SYBR FAST Universal qPCR Kit (KapaBiosystems). The pool was mixed with 2% of PhiX control (Illumina) and sequenced using MiSeq Reagent Kit V3–600 on the Illumina MiSeq Platform (Illumina Inc., San Diego, USA).

Bioinformatics

Reads were assigned to each of the 36 samples according to a unique barcode. Using a Mothur v.1.40.5 (last update 06/19/2018) pipeline all raw read pairs were joined at the overlapping region and contigs were then filtered following several steps, consisting in removing homopolymers, ambiguous sequences, sequences with an inappropriate length and artefacts (less than 10 sequences in the dataset (Schloss et al. 2009). OTUs were assembled using metrics to determine the quality of clustering with the Opticlust algorithm at a distance of 0.03. Taxonomic assignments were made with the SILVA ribosomal RNA databases v1.3.8 (Dec 16, 2019) (Quast et al. 2013). Samples were rarefied at the smallest number of sequences detected in a sample (3326) using “sub.sample” function in Mothur. Alpha diversity indices (Chao1 estimation, Shannon diversity index, and Shannon evenness index) and “Good's coverage” were calculated using function “summary.single” in Mothur. The coverage was calculated using the following equation: $C = [1 - (n/N)] * 100$ (%), where “n” is the number of OTUs and “N” the number of sequences (Good 1953), allowing a verification that the sequencing depth allowed satisfactory coverage of the bacterial communities in our samples. Venn diagrams were calculated and drawn using the “venn” function in Mothur.

Statistical analyses

We used the R version 4.2.0 (latest update 02/22/2022) (R Core Team 2019). A 2-dimensional non-metric multi-dimensional scaling (NMDS) plot was calculated using the “meta- MDS” function in the “vegan” package using Bray–Curtis distance. We used the “anosim” function in the “vegan” package to perform an ANalysis Of SIMilarities (ANOSIM) to statistically decide if groups were meaningful in the model. We obtained a *P*-value (*i.e.*, significance levels of the test) and a *R*-value (*i.e.*, between 0 and 1, close to 1 it implied a total dissimilarity between the groups tested). Variance analysis was carried out on all data using one-way ANOVA (Duncan test with a confidence interval of 95%). Normality tests and k-sample comparison of variances were also analyzed. These statistical analyses were carried out on XLSTAT software (XLSTAT 2015.2.01.16520, <http://www.xlstat.com>). The metabolic functions of the OTUs were predicted using the Tax4Fun package (Abhauer et al. 2015), which transforms the SILVA based OTUs into a taxonomic KEGG profile (Kyoto Encyclopedia of Genes and Genomes) organisms (fctProfiling=T), normalized by the 16S rRNA copy number (normCopyNo=T). Duncan and Kruskal–Wallis tests were performed on predictive functions to highlight any significant differences between the different seed populations at p -value < 0.05. The principal component analyses (PCA) were performed using the FactomineR package (v.2.4) (graphic and the confidence ellipses with a confidence interval of 95% were plotted using the Factoshiny package v2.4). Following PCA analysis, a Wilks test was performed to assess if treatments explained the distance between individuals. Data were analyzed using R Studio (v. 2022.07.1 Build 5.5.4).

Network analyses

Correlation networks were built using the bacterial 16S rRNA gene amplicon sequencing data. This was done with the aim of evaluating the impact of the soil Ni-concentration on the cohesion and complexity of the identified bacterial populations (no matter their origin: rhizosphere, plant roots and shoots) and their putative interactions. To do so, Spearman’s rank correlations were calculated for each dose between each pair of OTUs representing more than 0.1% of

the total bacterial community. This step of filtering out the infrequent OTUs was performed to increase the sensitivity of the resulting networks, as recommended by Berry and Widder (2014). The *p*-values correlations obtained were corrected using the Benjamini–Hochberg correction, to control for any false discovery rate upon multiple comparisons (Haynes 2013). Only the highly significant correlations, *i.e.* with a p -value ≤ 0.001 and a $|R|$ coefficient ≥ 0.5 were then retained to build the networks. For each network obtained, topological features were calculated to evaluate its complexity and connectivity. The number of nodes (*i.e.* OTUs with at least one highly significant correlation with another) and edges (highly significant correlations), the number of positive and negative edges, the positive to negative ratio (which indicates the balance between facilitative and inhibitive relationships within the network (Karimi et al. 2019), the number of modules (a group of OTUs highly connected) and the modularity, both linked to the functioning and robustness of the studied microbial process, which quantifies the extent to which the network can be broken up into smaller components (Röttgers and Faust 2018), the mean distance (or average path length, *i.e.* the average number of steps/distance along the shortest paths for all possible pairs of nodes), the clustering coefficient, (which represents the level of interactions among microorganisms), and the average degree, (which indicates the average level of microbial interaction in the network) were then used and compared in our study. For the last two indicators (clustering coefficient and average degree), statistical significance (with a p -value ≤ 0.05) was calculated using the Kruskal–Wallis test. Network correlations, topological features and statistical analysis were performed using R (v 4.2.0, (R Core Team 2019)), RStudio (v2022.02.2) and the igraph package (<http://igraph.org>). Networks were visualized using the R Bioconductor package RCy3 (v2.4.4, (Gustavsen et al. 2019)) and Cytoscape (v3.9.1).

Results

Physicochemical properties and enzyme activities

The global impact of the different Ni doses tested on soil data (MBC, MBN, FDA activity, pH, C/N, available and pseudo-total elements) was performed by

Principal Component Analysis (PCA). The main plot represents 57.0% of the total variability (Fig. 1a, b). There was a clear discrimination of the treatments D0 and D2 along the second axis (Dim 2), which represented 16.6% of the total variability. Indeed, samples corresponding to the lower Ni-concentrations (D0; negative ordinates) were clearly discriminated from those corresponding to the higher Ni-concentrations (D2: positive ordinates) (Fig. 1a, b). Moreover, we observed a clear discrimination between D2 (negative abscissa) and D0 treatment (positive abscissa) along the first axis (Dim 1) which represented 40.4% of the total variability (Fig. 1a). High values of Ni-DTPA were correlated with the D2 treatment and the higher the concentrations of available Ni (Ni-DTPA), the lower were the MBC, MBN, pH and soil ratio C/N values (Fig. 1b). FDA activity, for its part, appeared to be correlated with D0-D1 treatments (Fig. 1b). Table S1 presents the soil physicochemical and biological properties of the three studied treatments. The pH was significantly higher in the D0-D1 treatments compared to D2, whilst the soil acidification observed at D2 (decreased of 0.2 pH unit) seemed to be limited. An increase in the Ni contamination level (D0 to D2) significantly reduced the MBC and C/N ratios. Conversely, a significant increase in BCF was observed (shoot and root/Ni total, BCF-S and BCF-R, respectively) as well as in Ni-DTPA concentrations.

No influence of the increase of the Ni contamination level was observed on MBN, FDA activity and TF. Concerning plants, two PCAs were performed on mineral element profiles for root and shoot (Supplementary Fig. S1 and S2). For roots (Supplementary Fig. S1a, b), the first two dimensions of analysis expressed 73.5% of the total dataset inertia and the variability explained by this plane was highly significant. This PCA illustrated that no clear discrimination could be observed between the different treatments. Even if, according to the Ni gradient, an increase of Cr, Al, Fe and Ni could be observed but only significant for Ni (Supplementary Table S2). For shoot (Fig. S2a, b), the first two dimensions of analysis expressed 70.1% of the total variability. The Wilks test p-value (0.022) indicated that the distance between individuals was explained by the treatment. Thus, concerning shoot mineral contents, treatments were discriminated along the second axis (Dim 2), by Ni uptake, with higher Ni concentrations for D1 and D2 treatments, and by Fe and Se, with higher concentrations in D0. Values of mineral content in roots and shoots are given in Tables S2 and S3.

Microbial analysis

After bioinformatic treatments, the bacterial communities of the 36 samples allowed the obtention of

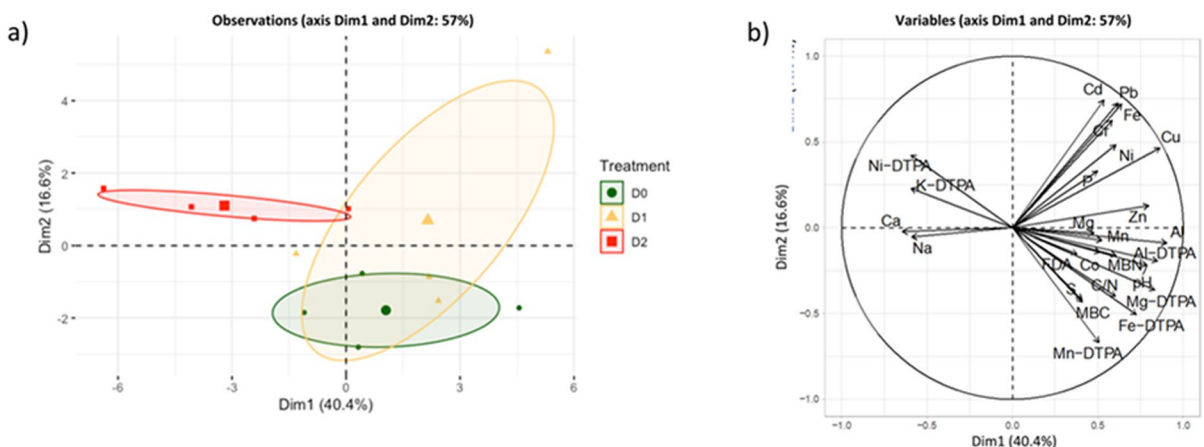


Fig. 1 Principal Component Analysis (PCA) generated from all measured soil parameters. **a**) Points represent the coordinate of different treatments (D0, D1 and D2) and refer to the treatments of D0 (control): Ni natural content, D1: natural content plus 20 mg Ni kg⁻¹ of dry soil, D2: natural content plus 80 mg Ni kg⁻¹ of dry soil. Confidence ellipses (95%) were drawn for

each treatment **b**) Soil parameters were measured at harvest and were included in the discrimination of samples. MBC and MBN (microbial biomass carbon and nitrogen, respectively), FDA (fluorescein diacetate activity), C/N ratio, pH, XX (total element) and XX-DTPA (soil available element)

116,424 effective sequences (3,234 reads for each sample) that were clustered into 2,234 OTUs. The Good's coverage index and the rarefaction curve analysis (data not shown) indicated that bacterial diversity was well represented.

Alpha diversity analysis revealed that species richness (Chao1 estimator) tended to decrease in the rhizosphere soil with higher levels of Ni

Table 1 Diversity indices

Code	Chao1 estimator	Shannon Index (H')	Shannon Evenness Index (SEI)
Shoot endosphere (SE)			
SE-D0	878 ± 78 a	3.08 ± 0.17 a	0.53 ± 0.01 a
SE-D1	591 ± 87 ab	2.86 ± 0.14 a	0.53 ± 0.02 a
SE-D2	377 ± 72 b	3.11 ± 0.12 a	0.51 ± 0.02 a
Root endosphere (RE)			
RE-D0	425 ± 25 a	2.17 ± 0.22 a	0.51 ± 0.02 a
RE-D1	386 ± 40 a	2.35 ± 0.24 a	0.44 ± 0.04 a
RE-D2	475 ± 66 a	1.97 ± 0.09 a	0.37 ± 0.02 a
Rhizosphere soil (RS)			
RS-D0	1013 ± 28 a	4.87 ± 0.06 a	0.74 ± 0.01 a
RS-D1	1307 ± 117 a	4.89 ± 0.07 ab	0.74 ± 0.01 a
RS-D2	964 ± 69 a	4.61 ± 0.01 b	0.72 ± 0.01 a

All diversity statistics were calculated using an OTU threshold of ≥ 97% sequence similarity on randomly sub-sampled data at the lower sample size (3,234 reads). Richness was calculated using the Chao1 estimator. Diversity was estimated from the Shannon–Wiener (H'), and Shannon Evenness Index (SEI) indices. Mean values ± standard error followed by the same letter are not significantly different according to Duncan's test at $p \leq 0.05$ ($n = 4$)

contamination (D2) compared to the D0 and D1 treatments (Table 1). For the shoot endosphere, this observation was even significant with a Chao1 estimator of 878 ± 78 for D0 and 377 ± 72 for D2. The Shannon Index was significantly lower in the rhizosphere soil at the D2 contamination level compared to the treatment D0, while in the root, the Shannon Evenness Index was lower at the D2 contamination level than for the D1 and D0 treatments.

A NMDS (Non-metric Multidimensional Scaling) graphical representation at OTU level allowed a comparison of the treatments (D0, D1 and D2) based on Bray–Curtis distance. This NMDS was carried out to compare dissimilarity of the bacterial community composition whatever the Ni-doses, considering all compartments together (rhizosphere soil, root and shoot endospheres) and resulted in a stress value of 0.063, which could be considered as “great” representation of the dataset in a reduced dimension (Supplementary Fig. S3). Indeed, stress < 0.05 provides an excellent representation in reduced dimensions, < 0.1 is great, < 0.2 is good and over 0.3 is insufficient (Clarke and Ainsworth 1993). There was a clear discrimination between samples only depending on the habitats studied (rhizosphere soil, root and shoot endospheres). Three other NMDS were carried out to assess the dissimilarity of the bacterial community composition independently in the three studied habitats (Fig. 2a, b, c). Concerning rhizosphere soils (Fig. 2a), this bidimensional representation revealed a stress value of 0.069, which makes it possible to exploit these results. D0 and D1 treatments were

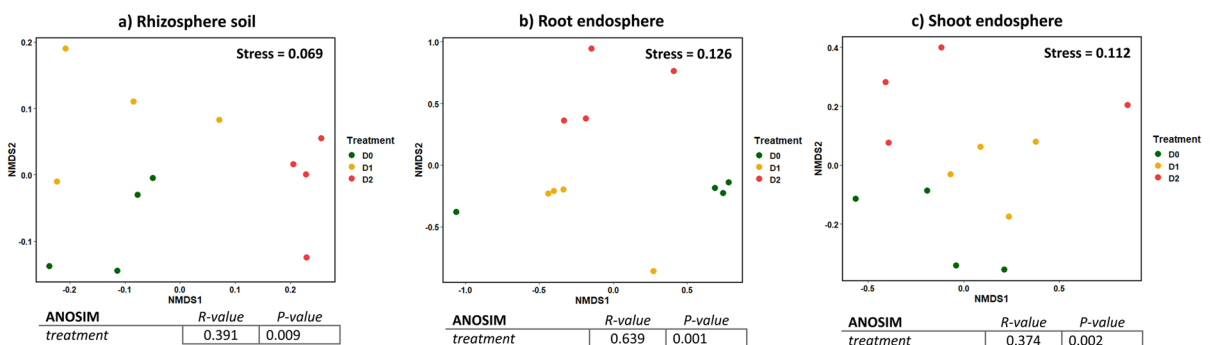


Fig. 2 Nonmetric multidimensional scaling (NMDS) ordination and analysis of similarities (ANOSIM) non-parametric statistical test, **a)** of the rhizosphere soil samples, **b)** of endosphere root samples, **c)** of endosphere shoot samples. Abbre-

viation D0, D1 and D2 corresponded to the following contamination levels with D0: (control) Ni natural content, D1: natural content plus 20 mg Ni kg⁻¹ of dry soil, D2: natural content plus 80 mg Ni kg⁻¹ of dry soil

clearly separated along NMDS1 from those corresponding to D2 treatments. In addition, D0 treatments were separated from D1 ones along NMDS2. Similarly, for root and shoot endospheres (Fig. 2b, c), a clear discrimination depending on the Ni contamination levels was observed with D0 and D1 treatments separated along NMDS2 from those corresponding to D2 treatments. The analysis of similarities (ANOSIM) non-parametric statistical test applied to the soil data revealed that the groups based on the contamination levels (D0, D1 and D2 treatments) were significantly explained by the dissimilarities between the samples (p -value = 0.009, R -value = 0.391). In the shoot endosphere, the same conclusions were drawn, although the power of explanation was lower than in the soil (p -value = 0.002, R -value = 0.374), while in the root endosphere, a higher power of explanation of the model was obtained (p -value = 0.001, R -value = 0.639).

Relative bacterial abundance at the class level is represented in Fig. 3a, b, c. In the rhizosphere soil, *Chloroflexi*.AD3 was the class the most abundant for the three treatments (D0, D1 and D2) (Fig. 3a). Their relative abundances increased significantly depending the Ni-doses from 35.3% (D0) to 51.0% (D2). Similarly, *Gammaproteobacteria* relative abundance was also higher for the D2 treatment in comparison with D0-D1. Conversely, *Saccharimonadia* abundances significantly decreased from D0 to D2 (31.1, 24.8 and 22.1%, respectively for D0, D1 and D2). In the same way, for the D2 treatment, we observed that the relative abundances of *Verrucomicrobia*, *Actinobacteria*, *Dehalococcoidia*, *Alphaproteobacteria* also significantly decreased.

The number of bacterial classes observed in the root and shoot endospheres were lower than those observed in the rhizosphere (Fig. 3b, c). In fact, we observed 11 classes in the rhizosphere (excluding

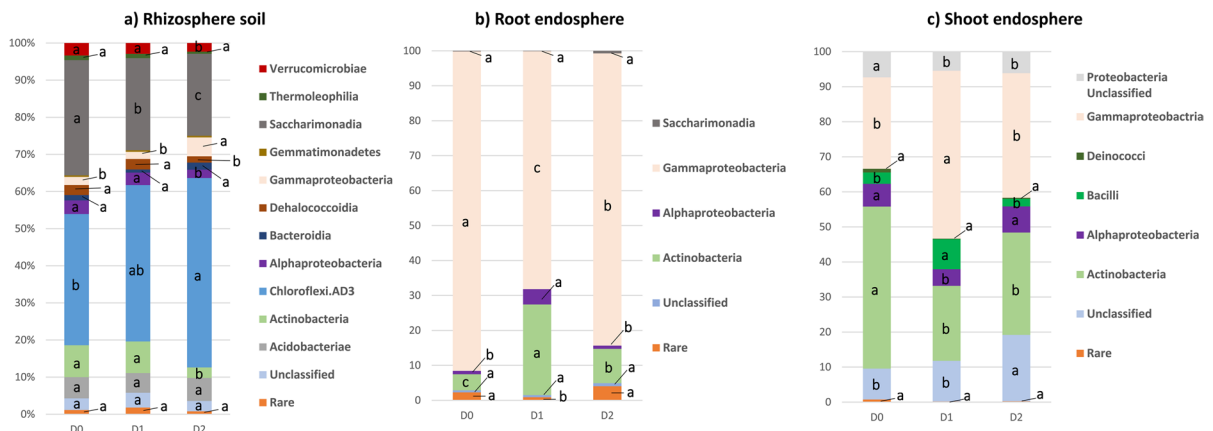


Fig. 3 Relative abundance of bacterial classes identified in the three habitats studied: **a)** rhizosphere, **b)** root endosphere and **c)** shoot endosphere (%). “Rare” refer to classes with less than 1% of relative abundance and were the following for the rhizosphere soil: *Abditibacteria*, *Acidimicrobiia*, *Bacilli*, *Chlamydiae*, *Chloroflexi*_unclassified, *Chloroflexia*, *Cyanobacteriia*, *Deinococci*, *Fimbriimonadia*, *Firmicutes*_unclassified, *Holophagae*, JG30-KF-CM66, *Ktedonobacteria*, *Lineage_IIb*, *Longimicrobia*, *Myxococcia*, OLB14, *Oligoflexia*, *Polyangia*, *Proteobacteria*_unclassified, RCP2-54_cl, *Subgroup_5*, TK10. They were the following for the root endosphere: *Abditibacteria*, *Acidimicrobiia*, *chloroflexi* AD3, *Bacteroidia*, *Bacteroidia* unclassified, *Chlamydiae*, *Chloroflexi*_unclassified, *Chloroflexia*, *Cyanobacteriia*, *Dehalococcoidia*, *Deinococci*, *Fimbriimonadia*, *Firmicutes*_unclassified, *Holophagae*, JG30-KF-CM66, *Ktedonobacteria*, *Lineage_IIb*, *Longimicrobia*, *Myxococcia*, OLB14, *Oligoflexia*, *Polyangia*, *Proteobacte-*

*ria*_unclassified, RCP2-54_cl, *Subgroup_5*, *Thermoleophila*, TK10, *Verrucomicrobiae*. They were the following for the shoot endosphere: *Abditibacteria*, *Acidimicrobiia*, *chloroflexi* AD3, *Bacilli*, *Bacteroidia*, *Bacteroidia* unclassified, *Chlamydiae*, *Chloroflexi*_unclassified, *Chloroflexia*, *Cyanobacteriia*, *Dehalococcoidia*, *Deinococci*, *Fimbriimonadia*, *Firmicutes*_unclassified, *Holophagae*, JG30-KF-CM66, *Ktedonobacteria*, *Lineage_IIb*, *Longimicrobia*, *Myxococcia*, OLB14, *Oligoflexia*, *Polyangia*, *Proteobacteria*_unclassified, RCP2-54_cl, *Subgroup_5*, *Thermoleophila*, TK10, *Verrucomicrobiae*. Abbreviation D0, D1 and D2 corresponded to the following contamination levels with D0: (control) Ni natural content, D1: natural content plus 20 mg Ni kg⁻¹ of dry soil, D2: natural content plus 80 mg Ni kg⁻¹ of dry soil. Means ± standard error followed by the same letter are not significantly different according to Duncan’s test at $p \leq 0.05$ ($n = 4$)

Rare and Unclassified OTUs), while only 4 and 6 classes were observed, respectively for the root and the shoot endosphere. In the case of the root endosphere (Fig. 3b), the main represented class corresponded to *Gammaproteobacteria*, with relative abundances between 68.1 and 91.4% depending the Ni-levels. The relative abundance of this class significantly decreased from D0 to D2. The second main classes represented in root endosphere were *Actinobacteria* and *Alphaproteobacteria*, which were the best-represented at the D1 treatment. *Chloroflexi*.AD3 and *Saccharimonadia*, which were the more represented in the rhizosphere, were not detected in root endosphere. Concerning shoot endosphere (Fig. 3c), among the 6 represented classes (excluding Rare and Unclassified OTUs), *Actinobacteria*, *Gammaproteobacteria* and *Bacilli* were the classes most present whatever the Ni-contamination level (respectively, mean of 32.3, 36.5 and 4.7% for their relative abundances). The relative abundance of *Actinobacteria*, *Proteobacteria* Unclassified and *Deinococci* decreased from D0 to D2. Moreover, as previously observed for root endosphere, no *Chloroflexi*.AD3 and *Saccharimonadia*, although the most-represented in the rhizosphere, were detected in shoot endosphere.

Based on OTU taxonomical assignment, Venn diagrams revealed bacterial OTUs which were specific or shared between the three Ni contamination levels in the three habitats studied (Fig. 4a, b, c). In each of these, bacterial OTUs that were specific to a contamination level represented only a small fraction of the

total relative abundance of the bacterial communities from the rhizosphere soil, root endosphere and shoot endosphere. For instance, the 64 rhizosphere-specific OTUs at the highest contamination level (D2) constituted 0.68% of the total relative abundance of the bacterial community from the rhizosphere soil (Fig. 4a). The 63 root-specific OTUs at D2 constituted 1.68% of the total relative abundance of the root endophytic bacterial community (Fig. 4b), and the 108 shoot-specific OTUs at D2 constituted 1.90% of the total relative abundance of the shoot endophytic bacterial community (Fig. 4c). Among the OTUs only found at the highest contamination level, most were unclassified. However, the most abundant genus identified in the rhizosphere soil with the higher Ni level belonged to the *Holophaga*, while in the root and shoot endosphere the most abundantly-identified OTUs specific to the highest contamination level belonged to *Saccharimonadales* spp.. In fact, most of the relatively abundant OTUs were those that were shared between the three contamination levels (D0, D1 and D2). Indeed, although the number of OTUs shared between the three habitats, these OTUs constituted a large part of the relative abundance of each of the three habitats. Indeed, these OTUs found in the center of each of the three diagrams correspond to the following ratio of OTUs: in the rhizosphere soil 171/492 (34.8%), in the root endosphere 48/244 (19.7%), and in the shoot endosphere 75/456 (16.4%). Nonetheless, they accounted for 96%, 98%, and 96% of the total relative

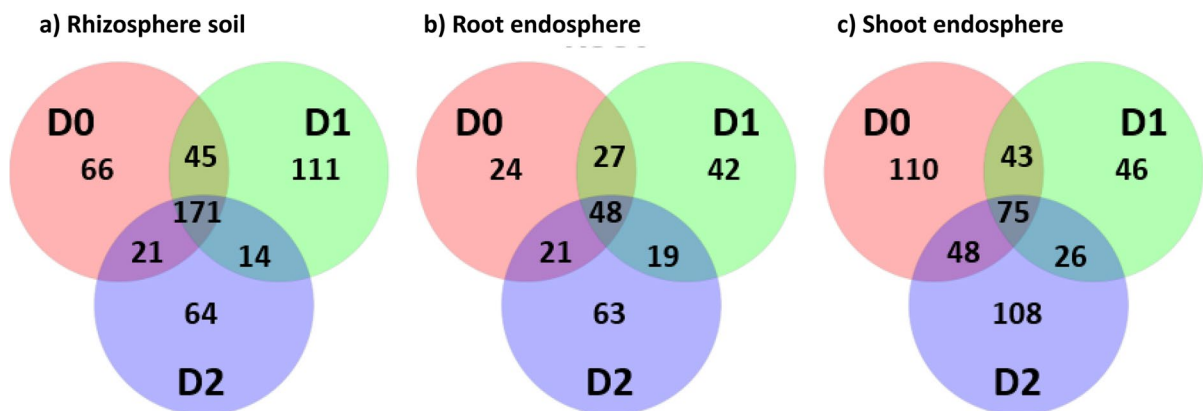


Fig. 4 Venn diagrams in the three habitats studied: **a)** rhizosphere soil, **b)** root endosphere and **c)** shoot endosphere showing bacterial OTU distribution at a 3% sequence dissimilarity

level among three contamination levels with D0: (control) Ni natural content, D1: natural content plus 20 mg Ni kg⁻¹ of dry soil, D2: natural content plus 80 mg Ni kg⁻¹ of dry soil

abundance in rhizosphere soil, in the root endosphere, and in the shoot endosphere, respectively. Moreover, focusing on those OTUs detected at the three contamination levels, several trends were visible (Supplementary Fig. S4). For instance, in the rhizosphere soil the relative abundance of OTUs of the genus *Chloroflexi* AD3 increased with the increase of Ni contamination levels (D0: 35.2%, D1: 42%, and D2: 51.0%), while conversely, *Saccharimonadales* spp. OTUs relative abundance decreased with the increase in Ni contamination levels (D0: 30.5%, D1: 24.9%, and D2: 22.0%). Even more drastic changes were observed in the root endosphere. For instance, the OTUs that belonged to the *Stenotrophomonas* genus increased with the rise in Ni contamination levels (D0: 0.62%, D1: 5.19%, and D2: 51.5%), while conversely, *Oxalobacteraceae* spp. OTUs relative abundance decreased with the increase in Ni contamination levels (D0: 65.9%, D1: 44.6%, and D2: 28.3%). With the increase in Ni contamination levels in the shoot endosphere, such trends were also revealed, with an increase of OTUs assigned to unclassified bacteria (D0: 12.1%, D1: 14.8%, and D2: 23.2%), while a decrease in OTUs that belonged to *Cutibacterium* (D0: 16.9%, D1: 12.4%, and D2: 8.3%) was observed. The relative abundance of the OTUs seemed to change depending on the contamination levels, and when grouped together by genus, some genera were found to be more competitive at the lower contamination levels, while this was the case for others at the highest contamination levels in the three habitats.

Network analyses

Using amplicon sequencing data, correlation networks were built and analyzed for each dose, in order to evaluate the impact of the soil Ni concentration on the complexity and cohesion of the rhizosphere and plant bacterial communities (Fig. 5). While no significant differences could be underlined regarding some topological features calculated for each correlation network produced (Table 2), a trend was nevertheless observed toward a perturbation of the bacterial cooperation by the Ni concentration increase in soil at D1 in comparison to D0. Indeed, a drastic increase in the network mean distance between D0 and D1 indicated that the bacterial community lost in terms of complexity, with fewer interactions (Table 2). This trend was strengthened by the concomitant decrease in the

network clustering coefficient between D0 and D1: the bacterial community at D0 was more dynamic and active than at D1. More inhibitive interactions could also be underlined at D1 in comparison to D0 due to the drastic decrease in the network positive to negative ratio (from 197.0 at D0 to 28.5 at D1).

In contrast, the decrease in the mean distance (from 2.9275 to 2.0614), the increase in the clustering coefficient (between 0.8176 ± 0.2309 to 0.8587 ± 0.1618), as well as of the positive to negative ratio (from 28.5 to 63.8) between D1 and D2, seemed to indicate that the bacterial community regained in complexity. Indeed, there were more numerous interactions with the more facilitative relationship within the studied community at high Ni concentration in soil (D2: natural content plus 80 mg Ni kg⁻¹ of dry soil).

The reorganization inside the bacterial community with the increasing level of Ni in soil could also be observed using the modularity, *i.e.* the structural organization of the networks studied in modules (groups of highly connected nodes). Indeed, the adjunction of Ni to the soil resulted in a decrease in the number of modules for D1 and D2 in comparison to D0 (Table 2 and Fig. 5). Interestingly, a specific independent module at D0 (highlighted in pale yellow in Fig. 5a) negatively interacted at D1 with some individuals of the main bacterial module (Fig. 5b). At D2 (Fig. 5c), its number of negative interactions with the main module drastically decreased, whilst at the same time some individuals were lost (putatively not adapted to the high Ni level).

Metagenome prediction

Metagenome prediction was applied to infer the metagenomic content of bacterial communities from the different habitats (rhizosphere soil, root and shoot endosphere) supplied with 3 different levels of Ni. This analysis was undertaken to evaluate the functional potential of the bacterial community metagenome from its 16S rRNA gene profile. We revealed 6 groups of level 1 KEGG Orthology (KO) in the communities belonging to the three habitats. In each habitat, the analysis predicted a higher proportion of functions related to metabolism (Fig. 6). Within the same habitat, the level of Ni contamination had no influence for the shoots' endophyte communities, but it did modulate the potential functions for the other two habitats (rhizosphere soil and root endosphere).

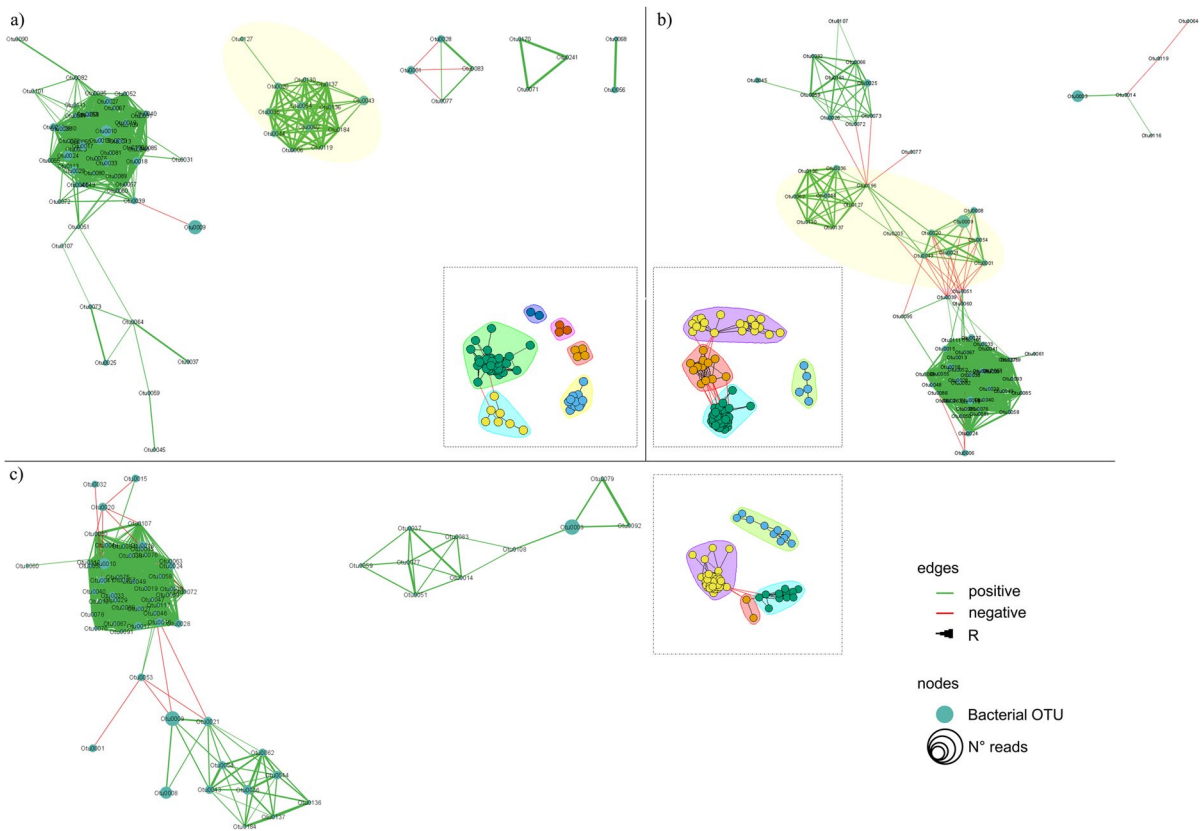


Fig. 5 Correlation networks at the OTU level: **a)** for D0 (control, Ni natural content of the soil), **b)** for D1 (natural content plus 20 mg Ni kg⁻¹ of dry soil) and **c)** for D2 (natural content plus 80 mg Ni kg⁻¹ of dry soil). Bacterial OTUs (nodes) are represented by a blue circle, the size of the circle being an indicator of the OTU read number. Edges (connections) between the nodes represent highly significant correlations

(p -value ≤ 0.001 and $|R| \geq 0.5$), in green when positive and in red when negative. The edge thickness is an indicator of the absolute value of R . For each network, identified ecological modules (group of OTUs strongly connected with each other) are presented with different colors in the dotted line square. Dynamics of a specific module according to the dose is underlined in pale yellow

Concerning the rhizosphere soil communities, it was at D1 (addition of 20 mg Ni kg⁻¹ of dry soil) that changes in predicted functions occurred. These functions were related to “organismal systems”, “human diseases”, “genetic information processing”, “environmental information processing” and “cellular processes”. For the root endosphere communities, differences could be underlined between D0 and D2 for the group functions of “organismal systems”, “environmental information processing”, and “cellular processes”.

Proceeding to a more detailed level of KO, we focused on the previous function groups at level 1 that showed significant differences within the same habitat depending on the level of Ni contaminations. Figure 7 presented the relative abundances greater

than 1% in the “cellular processes”, “environmental information processing”, “genetic information processing”, “organismal systems” and “human diseases” function groups for the bacterial communities of rhizosphere soil and/or root endosphere. In the rhizosphere soil, the predicted functions of the bacterial communities were similar for the D0 and D2 treatments, but different for the D1 treatment. The rhizobacterial communities in the soil of the treatment D1 showed an increase for predicted functions such as, “cellular community prokaryotes”, “cell growth and death”, “membrane transport”, “endocrine system”, “translation” “replication and repair” and “drug resistance” functions while, conversely, “cell motility”, “signal transduction”, “aging” and “folding, sorting and degradation” functions decreased

Table 2 Network topological features for each dose

Dose	No. of nodes	No. of edges	No. of positive edges	No. of negative edges	Positive to negative ratio	Modularity	No of modules	Mean distance	Clustering coefficient	Average degree
D0	77	792	788	4	197.0	0.1851	6	1.9294	0.8436 ± 0.2081 a	20.57 ± 15.29 a
D1	76	766	470	26	28.5	0.2388	4	2.9275	0.8176 ± 0.2309 a	20.16 ± 14.75 a
D2	65	713	702	11	63.8	0.1492	4	2.0614	0.8587 ± 0.1618 a	21.94 ± 14.92 a

Mean values ± standard error followed by the same letter are not significantly different according to Kruskal–Wallis test at p -value ≤ 0.05 ($n=12$). No: number

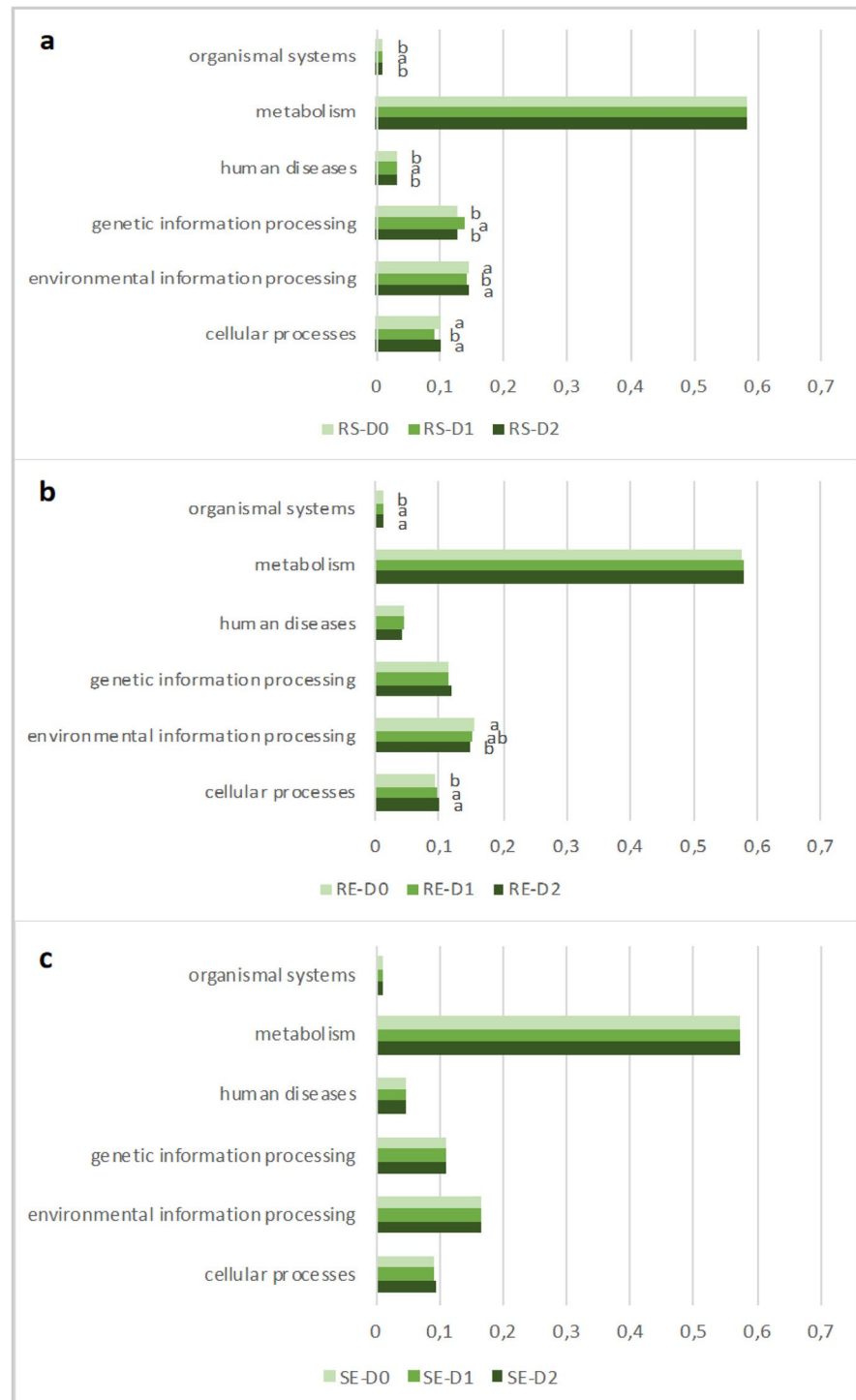
(Fig. 7a, c, e, g, h). For root endosphere communities, the Ni contamination level influenced the potentiality of functions, regardless of the treatment (D1 or D2), with an increase in “cellular community”, “cell motility”, “signal transduction”, “environmental adaptation”, and “endocrine system” functions and a decrease in “cell growth and death”, “membrane transport”, and “aging functions” (Fig. 7b, d, f).

Global analysis

Redundancy analysis (RDA) was performed between the soil parameters and the relative abundance (%) at the bacterial class level for the different treatments (Fig. 8a). The main plane (F1-F2), which explained 97.18% of the total variability clearly discriminated between D0, D1 and D2 treatments. D0 and D1 treatments were globally grouped in the left and the lower part of this graph, while D2 treatment appeared in the upper part of this representation. Spearman correlations ($p \leq 0.05$) were measured between the relative abundance of the bacterial classes and soil parameters for all the treatments (D0, D1 and D2). *Chloroflexi*.AD3 and *Gammaproteobacteria*, and to a lesser extent *Bacteroidia*, were more abundant in the rhizosphere soils of D2 treatments, which were correlated with high levels of Ni-DTPA (respectively, $R=0.57$, $R=0.70$ and $R=0.53$). Conversely, *Actinobacteria* (which is negatively correlated with Ni-DTPA; $R=-0.72$) and to a lesser extent *Saccharimonadia* were more abundant in the case of D0 and D1. *Actinobacteria* was mainly positively correlated to MB-C ($R=0.73$), MB-N ($R=0.37$), C/N ratio ($R=0.68$), pH ($R=0.70$). It seemed that more elements were available in the case of D0-D1 treatments than in the case of the D2 ones.

A further RDA was performed between the shoot and root parameters measured at the harvest and the relative abundance (%) of the dominant bacteria at the class level in root endosphere (R), and in shoot endosphere (S) (Fig. 8b). The main plane (F1-F2), which explained 97.91% of the total variability, clearly discriminated shoot (left part) and root (right part) endospheres, whatever the Ni-doses (D0, D1 and D2 treatments). Spearman correlations ($p \leq 0.05$) were measured between the relative abundance of the bacterial classes and element concentrations in shoots and roots for all the treatments (D0, D1 and D2). *Gammaproteobacteria* were more abundant

Fig. 6 Predicted metagenomic functions of bacterial community using Tax4Fun based on the 16S rRNA gene. The predicted relative abundance of groups KEGG ortholog (KO) in KEGG level 1 in rhizosphere soil (RS) (a), root endosphere (RE) (b) and in shoot endosphere (SE) (c). D0, D1 and D2 refer to the Ni treatments of D0 (control): Ni natural content, D1: natural content plus 20 mg Ni kg⁻¹ of dry soil, D2: natural content plus 80 mg Ni kg⁻¹ of dry soil. Means followed by the same letter are not significantly different according to Duncan's test at $p \leq 0.05$ ($n = 4$)



in the root endospheres whatever the Ni-doses considered and appeared inversely correlated with Ni concentrations in plant parts ($R = -0.53$). In contrast,

we observed a clear discrimination between shoot endospheric samples depending on the Ni-doses; D0-S treatments were clearly discriminated from

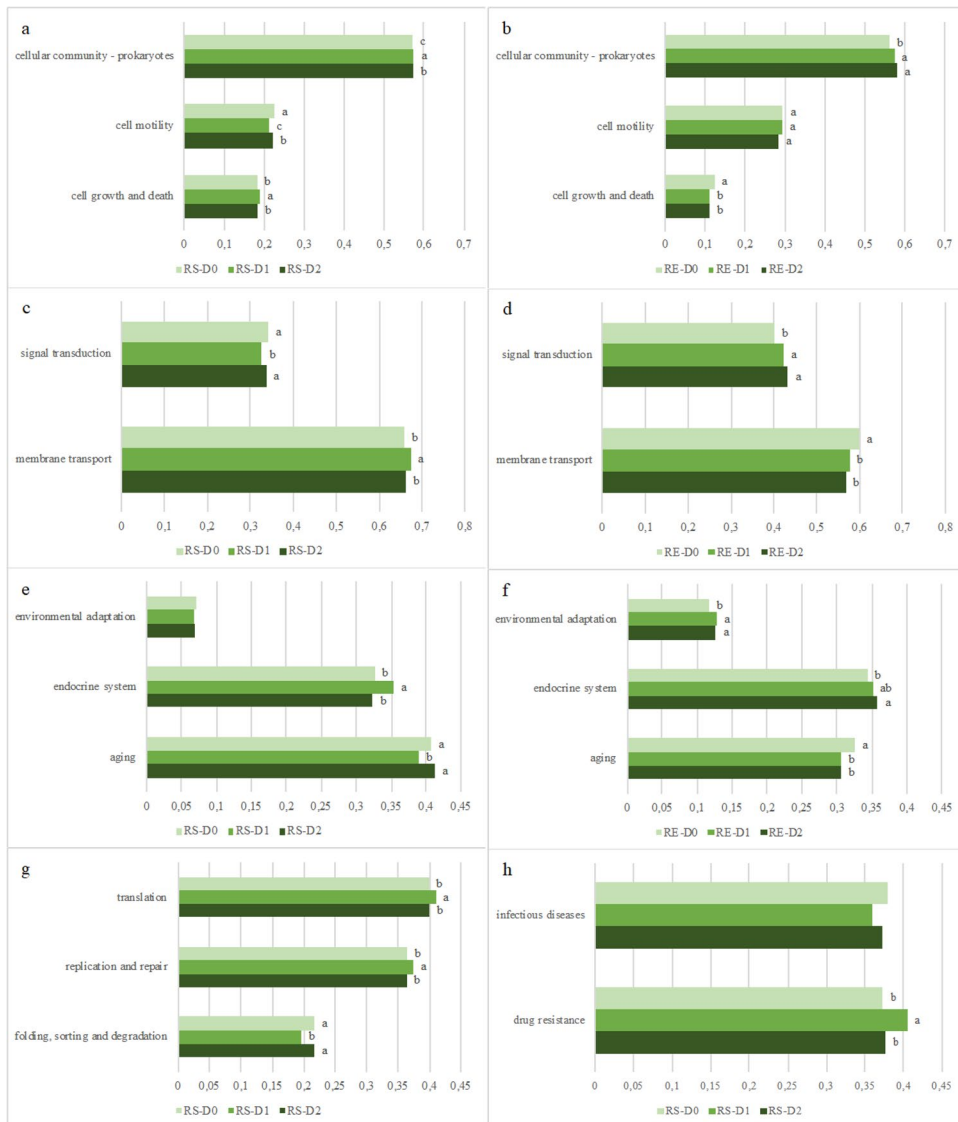


Fig. 7 Predicted metagenomic functions of the bacterial community using Tax4Fun based on the 16S rRNA gene. The predicted relative abundance > 1% of groups KEGG ortholog (KO) in KEGG level 2 for group functions of cellular processes in rhizosphere soil (RS) (a) and root endosphere (RE) (b), environmental information processing in rhizosphere soil (RS) (c) and root endosphere (RE) (d), organismal system in rhizosphere soil (RS) (e) and root endosphere (RE) (f), genetic

information processing in rhizosphere soil (RS) (g) and human diseases in rhizosphere soil (RS) (h). D0, D1 and D2 refer to the Ni treatments of D0 (control): Ni natural content, D1: natural content plus 20 mg Ni kg⁻¹ of dry soil, D2: natural content plus 80 mg Ni kg⁻¹ of dry soil. Means followed by the same letter are not significantly different according to Duncan's test at $p \leq 0.05$ ($n = 4$)

D1-S and D2-S ones. *Actinobacteria* was more abundant in the shoot endosphere for the D0 treatment and *Bacilli* and *Unclassified* bacteria in the shoot endosphere for the D1 and D2 treatments. These two classes were correlated with high Ni concentrations in plant parts (respectively, $R = 0.5$ and 0.70).

Discussion

Effect of Ni gradient on soil physicochemical properties and enzyme activities

The soil used in this study was sampled in the Melide

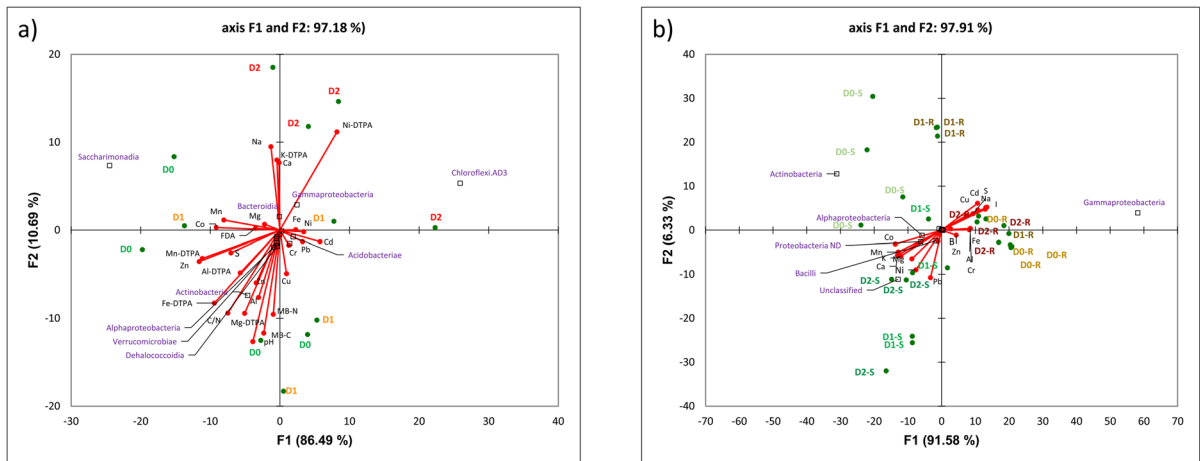


Fig. 8 Redundancy Analysis (RDA) performed between **a)** the soil parameters measured at the harvest and the relative abundance (%) of the dominant bacteria at the class level of rhizosphere communities from *Odontarrhena chalcidica* **b)** the shoot and root parameters measured at harvest, and the relative abundance (%) of the dominant bacteria at the class level in root endosphere (R), and in shoot endosphere (S). Dots are

observations and correspond to the different treatments (D0, D1 and D2) refer to the treatments of D0 (control): Ni natural content, D1: natural content plus 20 mg Ni kg⁻¹ of dry soil, D2: natural content plus 80 mg Ni kg⁻¹ of dry soil. MBC and MBN (microbial biomass carbon and nitrogen, respectively), FDA (fluorescein diacetate activity), C/N ratio, pH, XX (total element) and XX-DTPA (soil available element)

ultramafic complex (Spain) and was one of the networks of pilot-scale field sites of the Agronickel and Life-Agromine projects (Echevarria et al. 2017). In the context of European ultramafic region, this soil has both low total Ni concentration (850 mg Ni kg⁻¹) and available Ni concentration (Ni-DTPA: 19 mg Ni kg⁻¹), compared to other ultramafic soils found in other Spain areas or in Albania (total Ni concentration: 967 to 3140 mg Ni kg⁻¹ and Ni-DTPA: 37 to 124 mg Ni kg⁻¹, respectively in Spain (Eidián) and Albania (Pojskë)) (Echevarria et al. 2017; Kidd et al. 2018). In this study, we aimed to investigate the impact of a Ni concentration gradient on the soil's physicochemical properties and on the composition of the rhizosphere and endophytic bacterial communities of *O. chalcidica*. For that, the soil used was spiked with Ni sulfate in order to increase the Ni fraction: D1 corresponded to a doubling of the initial concentration of available Ni and D2 corresponded to 5 times the available Ni concentration to theoretically attain the same concentration gradient as that observed in Europe, from Spain (20 mg kg⁻¹), Austria (38.4 mg kg⁻¹) to Greece (71.1 mg kg⁻¹) (Kidd et al. 2018). At the end of the experiment, Ni-DTPA, corresponding to the potentially available Ni fraction (Rosenkranz et al. 2019), increased according to the

gradient dose. Our results showed: i) a lower soil Ni-DTPA at D1 compared to D2, but slightly higher than D0, ii) a significant increase of BCF in root and shoot at D1 and even more at D2 compared to D0, and iii) a reduction (not significant) of the translocation factor (TF) at D2 compared to D1 and even more compared to D0. This could be explained by an important Ni accumulation in root at D2 associated to a lower translocation to the shoot, which resulted in accumulation of extractable Ni-DTPA in the soil at D2 (Table S1). The increase in available Ni led to a detrimental effect on MBC or MBN, which were lower at D2 in comparison to D0. Our results were in accordance with those of Tang and McBride (2018), who showed that an increase of Ni-DTPA (from 1.02 to 86.9 mg kg⁻¹) in Ni-spiked soils induced a decrease of the microbial biomass. Shoot or root BCF increased according to the Ni gradient, which seemed to indicate that, when faced with an increase in available Ni, *O. chalcidica* took up more Ni from the soil. Our results were in line with those of Cui et al. (2012), who observed strong correlations between metal concentrations in wheat grain and metal concentrations in DTPA extracts. Comparing BCF (shoot or root) and TF, we showed an opposing trend according to the Ni gradient with an increase in BCFs and a decrease in TF. It

seemed that plants, at this vegetative stage, were able to accumulate bioavailable Ni in their roots in accordance with the Ni gradient, but that the Ni translocation from root to shoot parts was limited for the highest Ni concentrations.

In the roots, concerning major and minor elements, no difference was observed between treatments (see Supplementary Fig. S1 and Table S2), which indicated that absorption of these mineral elements by *O. chalcidica* was not affected by the treatment, except for Ni. Indeed, root Ni content increased significantly according to the treatment (D0 to D2). However, mineral contents in the shoots clearly showed a discrimination between treatments. Indeed, Ni might accumulate within roots, translocate to the shoots and may directly and/or indirectly impair various mineral nutrition processes, especially macro-or oligo-nutrient uptake (Amari et al. 2017). Ni uptake is mainly carried out by roots via a passive diffusion and/or active transport (Seregin and Kozhevnikova 2006) and enter via activated calcium and/or potassium channels in root cells (Boyd and Martens 1998; Verbruggen et al. 2009). Chen et al. (2009) showed that Ni has a similar character to Fe, leading it to compete with this element in uptake and following utilization in plant metabolism (Kidd et al. 2009). Likewise, Ni is reported to induce Fe deficiency, either by retarding its absorption or by causing its immobilization in roots (Myśliwa-Kurczel et al. 2004), which was in line with our results.

Effect of Ni gradient on soil bacterial community diversity

The rhizosphere, as well as plant tissues, harbor a wide variety of microorganisms, many of which can directly or indirectly enhance plant growth (Bulgarelli et al. 2013; Ling et al. 2022). A better description of taxonomic and functional diversity in the rhizosphere and endophytic microbiome and how they differ from each other, is crucial when manipulating them for sustainable ecosystem functioning. For instance, in constraining environments such as ultramafic soils, microorganisms from both rhizosphere and endosphere, have demonstrated their ability to increase plant survival and growth by alleviating metal toxicity and supplying nutrients to the plant (Benizri et al. 2021). However, heavy metals can affect the growth, morphology and metabolism of

microorganisms. Indeed, the main effects of exposure to metals are cell membrane disturbance and protein denaturation (Leita et al. 1995), albeit the effects of metals on the enzyme activity in the rhizosphere are complex, with some contrasting effects (Egamberdieva et al. 2010). With the increase of the Ni sulfate spiking doses, we found a decrease of fluorescein diacetate activity (FDA) known to be correlated with the overall enzyme activity (Schnürer and Rosswall 1982). Indeed, various enzymes, such as dehydrogenase, urease, and phosphatase, have been shown to be inhibited by Ni, along with the oxygen consumption of microbial communities (Li et al. 2018). Kandler and Böhm (1996) found that C-acquiring enzymes (cellulase, xylanase, b-glucosidase) were the least affected by soil pollution, while phosphatase and sulfatase were the most affected and finally, N-acquiring enzymes (urease) had an intermediate response. Nevertheless, elevated concentrations of trace elements in soils may lead to shifts in the culturable microbial size and diversity as well as their enzymatic activities (Barkay et al. 1985; Roane and Kellogg 1996). Since only a small percentage of microbes are culturable, new knowledge is needed for a holistic approach (Benizri and Kidd 2018). More recently, the development of sequencing techniques has improved our knowledge of the rhizosphere and endophytic microbiome of hyperaccumulating plants (Saad et al. 2018; Lopez et al. 2019a, b, 2020, 2022; Durand et al. 2021, 2022), but little is known of the responses of hyperaccumulating plant bacterial diversity to an elevated gradient of Ni.

Our previous work had demonstrated on hyperaccumulating plants that, first, the various plant organs and the bulk or rhizosphere soils sheltered different bacterial communities since the bacterial habitat is a major determinant of the diversity, and secondly, that soil properties may influence the bacterial diversity in soils and in plant organ endospheres, at the exception of seed endosphere (Durand et al. 2022). The current study confirmed this statement (Fig. 2): bacterial habitat was the main factor that influenced diversity, however for each habitat (rhizosphere, and root and shoot endospheres) Ni sulfate addition in the soil changed the bacterial community diversity.

Several elements corroborated our results, which revealed that microbial habitat was the main determinant to the bacterial diversity. Among the ecosystems, the soil harbors the highest microbial diversity

with commonly more than 2,000 species that can be identified within 0.5 g of soil (Uroz et al. 2010). Moreover, the root exudation is known to be a major factor that affects the structure of rhizosphere bacterial communities (Baudoin et al. 2003). In our study, the rhizosphere microbial communities were highly different from those of the endosphere, whatever the tested Ni-doses. Rhizodeposition might be one of the major process that selected this specific community. Various factors may also have been drivers explaining these contrasted community structures between habitats. They may be related to the endophytic competence (the ability to produce cell-wall degrading enzymes and the motility inside the host) (Compant et al. 2010), or related to the interaction with the host plant innate immune system (Jones and Dangl 2006), or even linked to tolerance to Ni concentration fluctuations in plant tissues (Bulgarelli et al. 2013). The OTU richness and OTU diversity (Table 1) were higher in the rhizosphere soil than in the endosphere samples. This clear trend of decreasing diversity and richness along the vertical axis (from soil to roots and shoots) suggested an active role of the plant in selecting specific bacterial taxa, which are more and more specialized, while moving from the below-ground to the aerial parts (Alibrandi et al. 2020).

Other studies have also corroborated the influence of Ni doses on bacterial communities in each of the three habitats studied. A long-term experiment (5 years) revealed that chronic exposure to Ni in soil entailed changes in the composition of the bacterial community, however the diversity indexes were unchanged (Li et al. 2015). In contrast, various studies had underlined that acute heavy metal contaminations caused by the spiking of metals in the soil led to a decrease in the microbial respiration and catabolic diversity of rhizosphere microorganisms (Frey and Rieder 2013; Xie et al. 2016). In addition, the impact of Ni seemed to be soil dependent and the shift in structure and composition in communities already adapted to Ni contaminated soils were less significant than non-adapted communities (Héry et al. 2003). The impact of the spiked-Ni gradient had already been tested on the rhizobacterial diversity of the two Ni-hyperaccumulating plants: *Rinorea cf. bengalensis* and *Phyllanthus rufuschaneyi* (Lopez et al. 2021). The authors showed significant decreases for the richness index but not for the diversity index, although they concluded that such changes in the rhizosphere

seemed plant dependent. In our study, in the rhizosphere soil, we observed a significant decrease in the Shannon Index (Table 1) from D0-D1 to D2, as well as a significant decrease in BMC (Table S1), while in root and shoot endosphere, the diversity (H') was not affected. This suggested that the Ni acute contamination has led to a perturbation of the structure and composition of the rhizobacterial communities.” To further investigate the composition of the bacterial community of the bacterial community’s structures in the three habitats studied (rhizosphere and root and shoot endosphere), under an elevated gradient of Ni, bar plots of the taxonomic distribution of classes were generated.

In the rhizosphere soil, we observed that *Chloroflexi*.AD3 was the dominant class for all three treatments (D0, D1 and D2) (Fig. 3a) with a significantly increase in its relative abundance according to the Ni-doses. The increased abundance of *Chloroflexi*.AD3 in metal-polluted sites, as found in our study, was in line with the observations by Chodak et al. (2013). The presence of this class suggested that it may be highly adapted to extreme environments and may play an important role in contaminated soils (Chodak et al. 2013). Moreover, *Chloroflexi* was also abundant in extreme and stressful conditions such as saline water (Yamada et al. 2005), geothermal soils (Yamada and Sekiguchi 2009) and/or acid mining drainage environments (García-Moyano et al. 2015; Mesa et al. 2017), which are characterized by high levels of available toxic metal species especially due to low pH. It was also found to be dominant in the rhizosphere of the hyperaccumulator plant *O. chacidica* growing on ultramafic soils from Northern Greece (Lopez et al. 2017) and in the rhizosphere of different hyperaccumulators collected on Halmahera Island (Indonesia) (Lopez et al. 2019b). This would suggest that these bacteria are effectively adapted to harsh environments such as the Ni-rich soils. *Gammaproteobacteria* is known to tolerate high Ni concentrations in metal-rich soils (Idris et al. 2006). Our results showed that this class was strictly linked to the soil Ni-DTPA in the RDA analysis (Fig. 8a). It seemed that the increase in soil Ni concentrations could favor this bacterial class. Likewise, Thompson and Wickham (2018) noticed a shift of the bacterial community structure with a dominance of *Gammaproteobacteria* in response to chromium-induced selective pressure, thereby showing the tolerance of this class of

soil bacteria to metal stress. Conversely, we observed a significant decrease in the relative abundances of *Verrucomicrobia*, *Actinobacteria*, *Saccharimonadia*, *Dehalococcoidia*, and *Alphaproteobacteria*. Our results confirmed those of Berg et al. (2012) and Luo et al. (2019), who observed a negative correlation between the relative abundance of *Verrucomicrobia* and pollution levels for metal-contaminated soils, thus showing that this class is sensitive to metal contamination. However, as this class contains only few cultivable species, their physiological roles in natural environments remain unknown (Rastogi et al. 2010). Concerning *Actinobacteria*, these bacteria are ubiquitous gram-positive bacteria with a number of important functions, including decomposition of all sorts of organic substances. This phylum is divided into six classes; of which *Actinobacteria* is one. The *Actinobacteria* class represents an important component of the microbial population in soils according to Polti et al. (2014). Indeed, their metabolic diversity and specific growth characteristics make them well-suited as agents for bioremediation (Cuozzo et al. 2011; Álvarez et al. 2012). Similarly, the biotechnological potential of *Actinobacteria* in the environment has been demonstrated by their ability to remove inorganic pollutants (Remenár et al. 2014). This is the reason why these bacteria have received special attention as candidates for this remediation technology. They are candidates of choice since they are able to thrive in either bulk soil or rhizosphere soil, or as epiphytes or endophytes associated to a wide spectrum of host plants (barley, wheat, rice, soybean, cowpea, chickpea, banana, tomato, and medicinal plants) (Sathya et al. 2017). In addition, bacteria belonging to this class are also known to be resistant to Ni. In their study, Costa et al. (2019) showed that among the bacteria strains isolated from ultramafic soils in Brazil, those belonging to the *Actinobacteria* phylum were predominant, ranging from 34 to 79% of the isolates identified. Moreover, testing the Ni-resistance (media enriched with NiSO_4) of isolated strains belonging to *Actinobacteria*, by an estimation of the highest concentration at which growth was still observed (defined as the maximum tolerable concentration; MTC), they observed high tolerance to Ni for the genus *Actinobacteria*. For example, the *Nocardia* genus was able to grow in the presence of up to 64 mM NiSO_4 , while *Streptomyces* did not grow at concentrations up to 8 mM NiSO_4 . The decrease in the *Actinobacteria*

relative abundance observed in our study particularly at the D2 dose (from 33.9% at D0-D1 doses to 29.2% at D2) could be explained by the fact that among the rhizobacteria belonging to this class, most failed to resist the D2 dose. The RDA performed between the soil parameters measured at the harvest and the relative abundance (%) of the dominant bacteria at the class level of rhizosphere communities from *O. chalcidica* (Fig. 8a) confirmed this hypothesis. Indeed, the greater the Ni-DTPA concentrations in the soil, the lower the relative abundance of *Actinobacteria* class was. We also observed a significant decrease in *Saccharimonadia* abundances from D0 to D2 as well as for *Dehalococcoidia* and *Alphaproteobacteria*. *Saccharimonadia* belongs to the phylum of *Patescibacteria*, formerly known as candidatus phylum TM7. This phylum is widespread in both natural and engineered ecosystems, but despite the widely-observed predominance of *Patescibacteria* in subsurface communities, their ecophysiology is poorly understood. Groundwater environments contained a high abundance of *Patescibacteria*, up to 38% of the total microbiomes (Kumar et al. 2017). Among them, the *Saccharimonadia* class has been shown to be highly abundant in soil and to have a potential for the metabolization of sugar compounds within plant tissues under oxic and anoxic conditions (Beckers et al. 2017; Herrmann et al. 2019) and hence might be adapted to soils or near-surface habitats. Shakya et al. (2013) have already reported a large variability in the relative abundance of *Saccharibacteria* under both biotic and abiotic stress. They were suggesting an important sensitivity of this taxon to variations in their environments, which is corroborated by our results as this taxon seemed very sensitive to Ni concentrations in soils. The factors that lead to this sensitivity are not well determined, but Shakya et al. (2013) suggested that they may be related to nutritional requirements, microbes-microbes or microbes-plants interactions. These observations could explain why in our study, this class decreased at the higher Ni-dose. To our knowledge we have been the first to describe that the *Dehalococcoidia* class that belongs to *Chloroflexota* phylum were less abundant when available Ni increased in the soil (Parks et al. 2018). *Alphaproteobacteria* are composed of both sensitive and non-sensitive species. Nonetheless, in benthic sediment where bacterial communities are chronically exposed to Ni from the erosion of ultramafic rocks, a study

revealed more negative than positive correlations between relative abundances of alphaproteobacterial species and sediment Ni concentrations (Gillmore et al. 2021). Otherwise, acute exposure to Ni in soils has been studied and resulted in a significant decrease in the *Alphaproteobacteria* class (Bararunyeretse et al. 2019).

Endophytic bacteria in plant organs are not randomly distributed and some dominant classes appear to be tissue- or organ-specific (Alibrandi et al. 2020). Indeed, concerning root and shoot endophytic bacteria, we observed respectively four and six major classes underlying a lower diversity in plant tissues in comparison with rhizosphere soils. These results were in accordance with the general views of endophytic colonization (Beckers et al. 2017). In fact, root exudates produced by the host plant in the rhizosphere soil led to the formation of distinctive, very rich and diverse rhizosphere microbiomes (Walker et al. 2003; Baudoin et al. 2003). The systemic colonization of a plant rest on the ability to survive and pass through the various barriers (immune or physical) inside the plant (Hardoim et al. 2008; Compant et al. 2010). These selective barriers could explain the great loss of diversity and evenness (Table 1) from rhizosphere soil to endophytic habitats. The two main classes found both in roots and shoots, whatever the Ni-dose tested, were *Gammaproteobacteria* and *Actinobacteria* (respectively, means of 81.0 and 13.4% in root endosphere and 36.5 and 32.3% in shoot endosphere). In fact, among *Actinobacteria*, members of *Streptomyces*, *Mycobacterium*, *Corynebacterium*, *Nocardia*, and *Rhodococcus* genus that are renowned for their metabolic capabilities and toxic metal resistance, as well as their large genomes and megaplasmids (Martínková et al. 2009; Presentato et al. 2020). Among *Streptomyces*, the species *Streptomyces acidiscabies* E13 is known to have plant growth promoting properties under nickel stress (Dimkpa et al. 2008).

Understanding of the bacterial interactions

Our results showed that the relative abundances of bacterial phyla in communities covaried with various environmental parameters and were notably correlated to available Ni (Ni-DTPA) (Fig. 8a) and to Ni accumulated in plant parts (Fig. 8b). These changes were related to habitats and treatments. Indeed, according to the treatment (D0 to D2), the

composition of the bacterial communities in each of the three habitats changed, revealing that the perturbation following Ni spiking was enough to change the bacterial community composition (Figs. 3 and 4). In fact, by observing the changes in relative abundance of the genera that were found in the three treatments, we observed a transition of the most abundant members of the communities in each habitat (Supplementary Fig. S3). A network analysis (Fig. 5) seemed relevant to detect the structural changes that could result from the disruption of interactions in the bacterial community.

The network-based approach is a powerful concept for studying the complex relationships between populations inside an ecosystem (Matchado et al. 2021). Indeed, it allows hypotheses to be derived from the massive high-throughput sequencing data sets (Röttjers and Faust 2018), and provides a better understanding of the microbial interactions, which can be reached by identifying co-occurrences or correlations. Association networks can open the way towards global models of ecosystem dynamics and this will allow predictions of the outcome of community alterations and the effects of perturbations (Faust and Raes 2012). By comparing networks/interactions between organisms from different environments, or from the same environment but before and after a perturbation, this approach allows to emphasize the response of the studied community structure to environmental changes. The correlation network study conducted in this work showed modifications in the level of interaction inside the bacterial community from the rhizosphere and the endosphere of *O. chalcidica* according to the amount of Ni. While D0 and D2 were characterized by a more stable and highly interacting community, D1 was more transient. Indeed, it seemed that for the D1 treatment, two bacterial sub-communities, one adapted to “low” Ni-content and the other adapted to higher Ni-content, coexisted. The high number of negative correlations at D1 treatment suggested competition between these two sub-communities.

Potential resistance of bacteria to high Ni-concentrations

Several processes can confer metal resistance to bacteria, and occur either before or after any internalization of the metal. Among the different mechanisms

involved upstream, it is possible to list the biosorption of metals on the cell membrane, and the synthesis of organic (*e.g.* exopolymers) or inorganic (*e.g.* metabolites) compounds to limit solubility and their consequent internalization within the cell. If the internalization takes place through specialized transport proteins, the metal can either be released into the environment by an active efflux process, or be sequestered in an inert form to limit its toxicity (Valls and De Lorenzo 2002; Chardot et al. 2005). In our study, no difference was found regarding the predicted functions for the shoot endospheric bacterial communities, whereas shoot Ni content varied from 1200 to more than 4000 mg Ni kg⁻¹ dry mass. Hyperaccumulating plants may possess microorganisms specialized in metal resistance (Benizri et al. 2021) and this was evidenced by the high relative abundance of predicted functions related to the “environmental information processing”. This category includes activities related to efflux systems and membrane transport proteins involved in Ni tolerance. Conversely, differences can be underlined for rhizosphere soil and root endospheric communities for the “environmental information processing functions”. For rhizosphere soil and root endospheric communities, we were able to demonstrate an increase in predicted functions related to quorum sensing (included in “cellular community – prokaryotes” functions) at high Ni concentrations, providing bacteria with greater resistance to heavy metals (Teitzel and Parsek 2003; Sarkar and Chakraborty 2008).

Finally, our results support the hypothesis that an increase in the available Ni in soil not only implies changes in the structure and diversity of bacterial communities associated to the rhizosphere and to the endosphere of *O. chalcidica*, but entails also changes in the predicted functions, particularly for the rhizosphere and root endospheric bacterial communities. The networks topological features studied seemed to indicate that the bacterial community was more stable at the lowest (D0) and the highest (D2) Ni soil contamination levels than at the intermediate level (D1). Indeed, the rhizosphere and endophytic bacterial community at D1 seemed to be composed of microbes adapted to low Ni concentration cohabiting with microbes which are more adapted to high Ni soil content. This resulted in a perturbation of the bacterial interactions and network by further competition between these two sub-communities. In the

same way, most of the predicted metagenomic functions also appeared to be different for D1 treatment in comparison with D0 and D2 ones. Endophytes are very important biological resources, which need to be explored in the future to achieve targets of environmental sustainability. The need is to investigate both the genomics and the integrated metabolism of the plant-endophyte relationship in order to garner benefits from this remarkable association.

Conclusion

Recently, the concept of microbe-assisted agromining has been introduced to underline the role of plant-associated microorganisms, both rhizosphere and endophytic, in metal bioavailability and uptake by host plants. However, the efficiency of plant-associated bacterial communities depends on a complex array of interacting factors, including soil metal concentration. A better understanding of the impact of different soil contamination levels of nickel on the structure and diversity of rhizosphere and endospheric bacterial communities is needed. We report in this study that an increase in the available nickel in soil induced shifts in the microbial community’s structure and functions, depending of the gradient of soil nickel availability in the soil. This increase not only induced changes in the dominant bacterial genera in the communities of the rhizosphere soil, but also in the root and shoot endosphere. Given our finding, increase in available nickel also entailed changes in the relative abundance of the bacterial predicted functions. In addition, topological features of the bacterial networks seemed to indicate that at an intermediate level of nickel contamination, two coexisting bacterial sub-communities were in competition, one adapted to “low” soil nickel content and the other to higher nickel content, while the bacterial communities were more stable at the lowest and the highest nickel soil contamination levels. These results, obtained under controlled conditions, highlighted the effect of soil Ni concentration on the rhizosphere and endospheric diversity of bacterial communities. However, it remains to be seen if these changes, depending of nickel soil contamination levels and observed in the rhizosphere and endosphere of *O. chalcida* were common in the case of other Ni-hyperaccumulators; this is an interesting avenue for future work.

Acknowledgements The authors thank Lucas Charrois for his assistance in the laboratory work, as well as Dr. Mathis Wolter for his precious help to assess the microbial community structure and diversity. We would like to thank members of the Experimental phytotronic platform of Lorraine PEPLor, Université de Lorraine, France for his technical assistance.

Author contributions Emile Benizri and Alexis Durand designed the research. Emile Benizri, Alexis Durand and Pierre Leglize performed research and analyzed the data. Alexis Durand, Séverine Lopez and Xavier Goux performed the molecular work, performed bioinformatics data analyses, and generated the figures. Emile Benizri wrote the first draft of the manuscript, and all authors commented on successive manuscript versions. All authors read and approved the final submission.

Declarations

Human and animal rights and informed consent This article does not contain any studies with human participants or animal performed by any of the authors.

Conflict of interest The authors declare that they have no known competing financial interests or personal relationships that could have appeared to influence the work reported in this paper.

References

- Abou-Shanab RI, Delorme TA, Angle JS, Chaney RL, Ghanem K, Moawad H, Ghazlan HA (2003) Phenotypic characterization of microbes in the rhizosphere of *Alyssum murale*. *Int J Phytoremediation* 5:367–79. <https://doi.org/10.1080/15226510309359043>
- Adam G, Duncan H (2001) Development of a sensitive and rapid method for the measurement of total microbial activity using fluorescein diacetate (FDA) in a range of soils. *Soil Biol Biochem* 33:943–951. [https://doi.org/10.1016/S0038-0717\(00\)00244-3](https://doi.org/10.1016/S0038-0717(00)00244-3)
- Afzal I, Shinwari ZK, Sikandar S, Shahzad S (2019) Plant beneficial endophytic bacteria: mechanisms, diversity, host range and genetic determinants. *Microbiol Res* 221:36–49. <https://doi.org/10.1016/j.micres.2019.02.001>
- Ait Barka E, Nowak J, Clément C (2006) Enhancement of chilling resistance of inoculated grapevine plantlets with a plant growth-promoting rhizobacterium, *Burkholderia phytofirmans* strain PsJN. *Appl Environ Microbiol* 72:7246–7252. <https://doi.org/10.1128/AEM.01047-06>
- Alexander EB (1994) Serpentine soils mapped in California and southwestern Oregon. *Soil Horizons* 35:61. <https://doi.org/10.2136/sh1994.3.0061>
- Alibrandi P, Schnell S, Perotto S, Cardinale M (2020) Diversity and structure of the endophytic bacterial communities associated with three terrestrial orchid species as revealed by 16S rRNA gene metabarcoding. *Front Microbiol* 11:3207. <https://doi.org/10.3389/FMICB.2020.604964/BIBTEX>
- Álvarez A, Yañez ML, Benimeli CS, Amoroso MJ (2012) Maize plants (*Zea mays*) root exudates enhance lindane removal by native *Streptomyces* strains. *Int Biodeterior Biodegradation* 66:14–18. <https://doi.org/10.1016/J.IBIOD.2011.10.001>
- Amari T, Ghnaya T, Abdely C (2017) Nickel, cadmium and lead phytotoxicity and potential of halophytic plants in heavy metal extraction. *South African J Bot* 111:99–110. <https://doi.org/10.1016/J.SAJB.2017.03.011>
- Abhauer KP, Wemheuer B, Daniel R, Meinicke P (2015) Tax4Fun: Predicting functional profiles from metagenomic 16S rRNA data. *Bioinformatics* 31:2882–2884. <https://doi.org/10.1093/bioinformatics/btv287>
- Bani A, Echevarria G, Sulçe S, Morel JL (2015) Improving the agronomy of *Alyssum murale* for extensive phytomining: A five-year field study. *Int J Phytoremediation* 17:117–127. <https://doi.org/10.1080/15226514.2013.862204>
- Bani A, Echevarria G, Pavlova D, Shallari S, Morel JL, Sulçe S (2018) Element case studies: Nickel. In: Van der Ent A, Baker A, Echevarria G, Simonnot MO, Morel JL (eds) *Agromining: farming for metals - extracting unconventional resources using plants*. Springer, pp 221–232. https://doi.org/10.1007/978-3-319-61899-9_12
- Bararunyeretse P, Zhang Y, Ji H (2019) Molecular biology-based analysis of the interactive effect of nickel and xanthates on soil bacterial community diversity and structure. *Sustain* 11:3888. <https://doi.org/10.3390/SU1143888>
- Barbaroux R, Mercier G, Blais JF, Morel JL, Simonnot MO (2011) A new method for obtaining nickel metal from the hyperaccumulator plant *Alyssum murale*. *Sep Purif Technol* 83:57–65. <https://doi.org/10.1016/j.seppur.2011.09.009>
- Barkey T, Tripp SC, Olson BH (1985) Effect of metal-rich sewage sludge application on the bacterial communities of grasslands. *Appl Environ Microbiol* 333–337. <https://www.ncbi.nlm.nih.gov/pmc/articles/PMC238403/pdf/aem00148-0083.pdf>
- Barzanti R, Ozino F, Bazzicalupo M, Gabbriellini R, Galardi F, Gonnelli C, Mengoni A (2007) Isolation and characterization of endophytic bacteria from the nickel hyperaccumulator plant *Alyssum bertolonii*. *Microb Ecol* 53:306–316. <https://doi.org/10.1007/s00248-006-9164-3>
- Baudoin E, Benizri E, Guckert A (2003) Impact of artificial root exudates on the bacterial community structure in bulk soil and maize rhizosphere. *Soil Biol Biochem* 35:1183–1192. [https://doi.org/10.1016/S0038-0717\(03\)00179-2](https://doi.org/10.1016/S0038-0717(03)00179-2)
- Beckers B, Op De Beeck M, Weyens N, Boerjan W, Vangronsveld J (2017) Structural variability and niche differentiation in the rhizosphere and endosphere bacterial microbiome of field-grown poplar trees. *Microbiome* 5:25. <https://doi.org/10.1186/s40168-017-0241-2>
- Benizri E, Kidd P (2018) The Role of the rhizosphere and microbes associated with hyperaccumulator plants in metal accumulation. In: Van der Ent A, Baker A, Echevarria G, Simonnot MO, Morel JL (eds) *Agromining: Farming for metals - Extracting unconventional resources using plants*. Springer, pp 157–188. https://doi.org/10.1007/978-3-319-61899-9_9

- Benizri E, Lopez S, Durand A, Kidd P (2021) Diversity and role of endophytic and rhizosphere microbes associated with hyperaccumulator plants during metal accumulation. In: Van der Ent A, Baker A, Echevarria G, Simonnot MO, Morel JL (eds) *Agromining: Farming for metals - Extracting unconventional resources using plants*. Springer, pp 239–279. <https://doi.org/10.1007/978-3-030-58904-2>
- Berg J, Brandt KK, Al-Soud WA, Holm PE, Hansen LH, Sørensen SJ, Nybroe O (2012) Selection for Cu-tolerant bacterial communities with altered composition, but unaltered richness, via long-term Cu exposure. *Appl Environ Microbiol* 78:7438–7446. <https://doi.org/10.1128/AEM.01071-12/FORMAT/EPUB>
- Berry D, Widder S (2014) Deciphering microbial interactions and detecting keystone species with co-occurrence networks. *Front Microbiol* 5:1–14. <https://doi.org/10.3389/fmicb.2014.00219>
- Boyd RS, Jaffré T (2009) Elemental concentrations of eleven new caledonian plant species from serpentine soils: Elemental correlations and leaf-age effects. *Northeast Nat* 16:93–110. <https://doi.org/10.1656/045.016.0508>
- Boyd RS, Martens SN (1998) Nickel hyperaccumulation by *Thlaspi montanum* var. *montanum* (*Brassicaceae*): a constitutive trait. *Am J Bot* 85:259–265. <https://doi.org/10.2307/2446314>
- Brookes PC, Kragt JF, Powlson DS, Jenkinson DS (1985) Chloroform fumigation and the release of soil nitrogen: The effects of fumigation time and temperature. *Soil Biol Biochem* 17:831–835. [https://doi.org/10.1016/0038-0717\(85\)90143-9](https://doi.org/10.1016/0038-0717(85)90143-9)
- Bulgarelli D, Schlaeppi K, Spaepen S, Van Themaat EVL, Schulze-Lefert P (2013) Structure and functions of the bacterial microbiota of plants. *Annu Rev Plant Biol* 64:807–838. <https://doi.org/10.1146/annurev-arpla-nt-050312-120106>
- Cabello-Conejo MI, Becerra-Castro C, Prieto-Fernández A, Monterroso C, Saavedra-Ferro A, Mench M, Kidd PS (2014) Rhizobacterial inoculants can improve nickel phytoextraction by the hyperaccumulator *Alyssum pinto-dasilvae*. *Plant Soil* 379:35–50. <https://doi.org/10.1007/s11104-014-2043-7>
- Chaney RL, Angle JS, Broadhurst CL, Peters CA, Tappero RV, Sparks DL (2007) Improved understanding of hyperaccumulation yields commercial phytoextraction and phytomining technologies. *J Environ Qual* 36:1429–1443. <https://doi.org/10.2134/jeq2006.0514>
- Chaney RL, Chen KY, Li YM, Angle JS, Baker AJM (2008) Effects of calcium on nickel tolerance and accumulation in *Alyssum* species and cabbage grown in nutrient solution. *Plant Soil* 311:131–140. <https://doi.org/10.1007/s11104-008-9664-7>
- Chaney RL, Baker AJM, Morel JL (2018) The long road to developing agromining/phytomining. In: *Agromining: Farming for Metals*. In: Van der Ent A, Baker A, Echevarria G, Simonnot MO, Morel JL (eds) *Agromining: Farming for metals - Extracting unconventional resources using plants*. Springer, pp 1–17. https://doi.org/10.1007/978-3-319-61899-9_1
- Chardot V, Massoura ST, Echevarria G, Reeves RD, Morel J-L (2005) Phytoextraction potential of the nickel hyperaccumulators *Leptoplax emarginata* and *Bornmuellera tymphaea*. *Int J Phytoremediation* 7:323–335. <https://doi.org/10.1080/16226510500327186>
- Chen C, Huang D, Liu J (2009) Functions and toxicity of nickel in plants: recent advances and future prospects. *Clean Soil Air Water* 37:304–313. <https://doi.org/10.1002/CLEN.200800199>
- Chodak M, Golebiewski M, Morawska-Płoskonka J, Kuduk K, Niklińska M (2013) Diversity of microorganisms from forest soils differently polluted with heavy metals. *Appl Soil Ecol* 64:7–14. <https://doi.org/10.1016/J.APSSOIL.2012.11.004>
- Clarke KR, Ainsworth M (1993) A method of linking multivariate community structure to environmental variables. *Mar Ecol Prog Ser* 92:205–219. <https://doi.org/10.3354/meps092205>
- Compant S, Reiter B, Nowak J, Sessitsch A, Clément C, Barka EA (2005) Endophytic colonization of *Vitis vinifera* L. by plant growth-promoting bacterium *Burkholderia* sp. strain PsJN. *Appl Environ Microbiol* 71:1685–1693. <https://doi.org/10.1128/AEM.71.4.1685>
- Compant S, Clément C, Sessitsch A (2010) Plant growth-promoting bacteria in the rhizo- and endosphere of plants: Their role, colonization, mechanisms involved and prospects for utilization. *Soil Biol Biochem* 42:669–678. <https://doi.org/10.1016/j.soilbio.2009.11.024>
- Corzo Remigio A, Chaney RL, Baker AJM, Edraki M, Erskine PD, Echevarria G, van der Ent A (2020) Phytoextraction of high value elements and contaminants from mining and mineral wastes: Opportunities and limitations. *Plant Soil* 449:11–37. <https://doi.org/10.1007/s11104-020-04487-3>
- Costa FS, Macedo MWFS, Araújo ACM, Rodrigues CA, Kuramae EE, de Barros Alcanfor SK, Pessoa-Filho M, Barreto CC (2019) Assessing nickel tolerance of bacteria isolated from serpentine soils. *Brazilian J Microbiol* 50:705–713. <https://doi.org/10.1007/S42770-019-00111-4/FIGURES/3>
- Cui L, Pan G, Li L, Yan J, Zhang A, Bian R, Chang A (2012) The reduction of wheat Cd uptake in contaminated soil via biochar amendment: A two-year field experiment. *BioResources* 7:5666–5676. <https://doi.org/10.15376/biores.7.4.5666-5676>
- Cuozzo SA, Fuentes MS, Bourguignon N, Benimeli CS, Amoroso MJ (2011) Chlordane biodegradation under aerobic conditions by indigenous *Streptomyces* strains. *Int Biodeterior Biodegradation* 66:19–24. <https://doi.org/10.1201/b14776-14>
- Dimkpa C, Svatoš A, Merten D, Büchel G, Kothe E (2008) Hydroxamate siderophores produced by *Streptomyces acidiscabies* E13 bind nickel and promote growth in cowpea (*Vigna unguiculata* L.) under nickel stress. *Can J Microbiol* 54:163–172. <https://doi.org/10.1139/W07-130/ASSET/IMAGES/W07-130T2H.GIF>
- Durand A, Piutti S, Rue M, Morel JL, Echevarria G, Benizri E (2016) Improving nickel phytoextraction by co-cropping hyperaccumulator plants inoculated by plant growth promoting rhizobacteria. *Plant Soil* 399:179–192. <https://doi.org/10.1007/s11104-015-2691-2>
- Durand A, Leglize P, Lopez S, Sterckeman T, Benizri E (2022) *Noccaea caerulea* seed endosphere: A habitat for an endophytic bacterial community preserved through generations and protected from soil influence. *Plant Soil*. <https://doi.org/10.1007/s11104-021-05226-y>

- Durand A, Sterckeman T, Gonnelli C, Coppi A, Bacci G, Leglize P, Benizri E (2021) A core seed endophytic bacterial community in the hyperaccumulator *Nocca caerulea* across 14 sites in France. *Plant Soil* 203–216. <https://doi.org/10.1007/s11104-020-04743-6>
- Echevarria G, Massoura ST, Sterckeman T, Becquer T, Schwartz C, Morel JL (2006) Assessment and control of the bioavailability of nickel in soils. *Environ Toxicol Chem* 25:643–651
- Echevarria G, Baker AJM, Benizri E, Morel JL, van der Ent A, Houzelot V et al (2015) Agromining for nickel: a complete chain that optimizes ecosystem services rendered by ultramafic landscapes. In *Mineral Resources in a Sustainable World*, Vol 1–5, eds AS Andre-Mayer AS, Cathelineau M, Muchez P (Nancy), 1465–1467
- Echevarria G, Bani A, Benizri E, Kidd PS, Kissler J, Konstantinou M, Tognacchini A (2017) LIFE agromine: A European demonstration project for Ni agromining. In: *The 14th International Phytotechnologies Conference*. Montreal, pp 25–29
- Echevarria G (2018) Genesis and behaviour of ultramafic soils and consequences for nickel biogeochemistry. In: *Agromining: Farming for Metals*. In: Van der Ent A, Baker A, Echevarria G, Simonnot MO, Morel JL (eds) *Agromining: Farming for metals - Extracting unconventional resources using plants*. Springer, pp 135–156. https://doi.org/10.1007/978-3-319-61899-9_8
- Egamberdieva D, Renella G, Wirth S, Islam R (2010) Enzyme activities in the rhizosphere of plants. 149–166. https://doi.org/10.1007/978-3-642-14225-3_8
- Faust K, Raes J (2012) Microbial interactions: From networks to models. *Nat Rev Microbiol* 10:538–550. <https://doi.org/10.1038/nrmicro2832>
- Frey B, Rieder SR (2013) Response of forest soil bacterial communities to mercury chloride application. *Soil Biol Biochem* 65:329–337. <https://doi.org/10.1016/j.soilbio.2013.06.001>
- García-Moyano A, Austnes AE, Lanzén A, González-Toril E, Aguilera Á, Øvreås L (2015) Novel and unexpected microbial diversity in acid mine drainage in Svalbard (78° N), revealed by culture-independent approaches. *Microorganisms* 3:667–694. <https://doi.org/10.3390/MICROORGANISMS3040667>
- Gillmore ML, Golding LA, Chariton AA, Stauber JL, Stephenson S, Gissi F, Greenfield P, Juillot F, Jolley DF (2021) Metabarcoding reveals changes in benthic eukaryote and prokaryote community composition along a tropical marine sediment nickel gradient. *Environ Toxicol Chem* 40:1892–1905. <https://doi.org/10.1002/ETC.5039>
- Glick BR (2005) Modulation of plant ethylene levels by the bacterial enzyme ACC deaminase. *FEMS Microbiol Lett* 251:1–7. <https://doi.org/10.1016/j.femsle.2005.07.030>
- Glick BR (2010) Using soil bacteria to facilitate phytoremediation. *Biotechnol Adv* 28:367–374. <https://doi.org/10.1016/j.biotechadv.2010.02.001>
- Good IJ (1953) The population frequencies of species and the estimation of population parameters. *Biometrika* 40:237–264. <https://doi.org/10.1093/biomet/40.3-4.237>
- Gustavsen JA, Pai S, Isserlin R, Demchak B, Pico AR (2019) RCy3: Network biology using Cytoscape from within R. *F1000Research* 8:1774. <https://doi.org/10.12688/F1000RESEARCH.20887.2>
- Hardoim PR, van Overbeek LS, van Elsas JD (2008) Properties of bacterial endophytes and their proposed role in plant growth. *Trends Microbiol* 16:463–471. <https://doi.org/10.1016/j.tim.2008.07.008>
- Haynes W (2013) Benjamini-Hochberg method BT. In: Dubitzky W, Wolkenhauer O, Cho K-H, Yokota H (eds) *Encyclopedia of systems biology*, Springer. Springer, New York, p 78
- Healey A, Furtado A, Cooper T, Henry RJ (2014) Protocol: A simple method for extracting next-generation sequencing quality genomic DNA from recalcitrant plant species. *Plant Methods* 10:21. <https://doi.org/10.1186/1746-4811-10-21>
- Herrmann M, Wegner CE, Taubert M, Geesink P, Lehmann K, Yan L, Lehmann R, Totsche KU, Küsel K (2019) Predominance of *Candida patescens* in groundwater is caused by their preferential mobilization from soils and flourishing under oligotrophic conditions. *Front Microbiol* 10:1407. <https://doi.org/10.3389/FMICB.2019.01407/BIBTEX>
- Héry M, Nazaret S, Jaffré T, Normand P, Navarro E (2003) Adaptation to nickel spiking of bacterial communities in neocaledonian soils. *Environ Microbiol* 5:3–12. <https://doi.org/10.1046/J.1462-2920.2003.00380.X>
- Idris R, Trifonova R (2004) Bacterial communities associated with flowering plants of the Ni hyperaccumulator *Thlaspi goesingense*. *Appl Environ Microbiol* 70:2667–2677. <https://doi.org/10.1128/AEM.70.5.2667>
- Idris R, Kuffner M, Bodrossy L, Puschenreiter M, Monchy S, Wenzel WW, Sessitsch A (2006) Characterization of Ni-tolerant methylobacteria associated with the hyperaccumulating plant *Thlaspi goesingense* and description of *Methylobacterium goesingense* sp. nov. *Syst Appl Microbiol* 29:634–644. <https://doi.org/10.1016/j.syapm.2006.01.011>
- Jones JDG, Dangl JL (2006) The plant immune system. *Nature* 444:323–329. <https://doi.org/10.1038/NATURE05286>
- Kandeler E, Böhm KE (1996) Temporal dynamics of microbial biomass, xylanase activity, N-mineralisation and potential nitrification in different tillage systems. *Appl Soil Ecol* 4:181–191. [https://doi.org/10.1016/S0929-1393\(96\)00117-5](https://doi.org/10.1016/S0929-1393(96)00117-5)
- Karimi B, Dequiedt S, Terrat S, Jolivet C, Arrouays D, Wincker P, Cruaud C, Bispo A, Chemidlin Prévost-Bouré N, Ranzard L (2019) Biogeography of soil bacterial networks along a gradient of cropping intensity. *Sci Rep* 9(1):1–10. <https://doi.org/10.1038/s41598-019-40422-y>
- Kembel SW, O'Connor TK, Arnold HK, Hubbell SP, Wright SJ, Green JL (2014) Relationships between phyllosphere bacterial communities and plant functional traits in a neotropical forest. *Proc Natl Acad Sci U S A* 111:13715–13720. <https://doi.org/10.1073/pnas.1216057111>
- Kidd P, Barceló J, Bernal MP, Navari-Izzo F, Poschenrieder C, Shilev S, Clemente R, Monterroso C (2009) Trace element behaviour at the root–soil interface: Implications in phytoremediation. *Environ Exp Bot* 67:243–259. <https://doi.org/10.1016/J.ENVEXPBOT.2009.06.013>
- Kidd PS, Bani A, Benizri E, Gonnelli C, Hazotte C, Kissler J, Konstantinou M, Kuppens T, Kyrkas D, Laubie B, Malina R, Morel JL, Olcay H, Pardo T, Pons MN, Prieto-Fernández Á, Puschenreiter M, Quintela-Sabaris C,

- Ridard C, Rodríguez-Garrido B, Rosenkranz T, Rozpadek P, Saad R, Selvi F, Simonnot MO, Tognacchini A, Turnau K, Wazny R, Witters N, Echevarria G (2018) Developing sustainable agromining systems in agricultural ultramafic soils for nickel recovery. *Front Environ Sci* 6:1–20. <https://doi.org/10.3389/fenvs.2018.00044>
- Kierczak J, Pietranik A, Pędziwiatr A (2021) Ultramafic geosystems as a natural source of Ni, Cr, and Co to the environment: A review. *Sci Total Environ* 755:142620. <https://doi.org/10.1016/J.SCITOTENV.2020.142620>
- Kumar KV, Singh N, Behl H, Srivastava S (2008) Influence of plant growth promoting bacteria and its mutant on heavy metal toxicity in *Brassica juncea* grown in fly ash amended soil. *Chemosphere* 72:678–683. <https://doi.org/10.1016/j.chemosphere.2008.03.025>
- Kumar KV, Srivastava S, Singh N, Behl HM (2009) Role of metal resistant plant growth promoting bacteria in ameliorating fly ash to the growth of *Brassica juncea*. *J Hazard Mater* 170:51–57. <https://doi.org/10.1016/j.jhazmat.2009.04.132>
- Kumar S, Herrmann M, Thamdrup B, Schwab VF, Geesink P, Trumbore SE, Totsche KU, Küsel K (2017) Nitrogen loss from pristine carbonate-rock aquifers of the hainich critical zone exploratory (Germany) is primarily driven by chemolithoautotrophic anammox processes. *Front Microbiol* 8:1951. <https://doi.org/10.3389/FMICB.2017.01951/BIBTEX>
- Lebeau T, Braud A, Jézéquel K (2008) Performance of bioaugmentation-assisted phytoextraction applied to metal contaminated soils: A review. *Environ Pollut* 153:497–522. <https://doi.org/10.1016/j.envpol.2007.09.015>
- Leita L, De Nobili M, Muhlbachova G, Mondini C, Marchiol L, Zerbi G (1995) Bioavailability and effects of heavy metals on soil microbial biomass survival during laboratory incubation. *Biol Fertil Soils* 19:103–108. <https://doi.org/10.1007/BF00336144>
- Li YM, Chaney RL, Brewer EP, Angle JS, Nelkin J (2003) Phytoextraction of nickel and cobalt by hyperaccumulator *Alyssum* species grown on nickel-contaminated soils. *Environ Sci Technol* 37:1463–1468. <https://doi.org/10.1021/es0208963>
- Li J, Hu HW, Ma YB, Wang JT, Liu YR, He JZ (2015) Long-term nickel exposure altered the bacterial community composition but not diversity in two contrasting agricultural soils. *Environ Sci Pollut Res* 22:10496–10505. <https://doi.org/10.1007/S11356-015-4232-1/FIGURES/6>
- Li H, Yao J, Gu J, Duran R, Roha B, Jordan G, Liu J, Min N, Lu C (2018) Microcalorimetry and enzyme activity to determine the effect of nickel and sodium butyl xanthate on soil microbial community. *Ecotox Environ Saf* 163:577–584. <https://doi.org/10.1016/j.ecoenv.2018.07.108>
- Lindsay WL, Norvell WA (1978) Development of a DTPA soil test for zinc, iron, manganese, and copper. *Soil Sci Soc Am J* 42:421–428. <https://doi.org/10.2136/sssaj1978.03615995004200030009x>
- Ling N, Wang T, Kuzyakov Y (2022) Rhizosphere bacteriome structure and functions. *Nat Commun* 13:1–13. <https://doi.org/10.1038/s41467-022-28448-9>
- Lopez S, Piutti S, Vallance J, Morel JL, Echevarria G, Benizri E (2017) Nickel drives bacterial community diversity in the rhizosphere of the hyperaccumulator *Alyssum murale*. *Soil Biol Biochem* 114:121–130. <https://doi.org/10.1016/j.soilbio.2017.07.010>
- Lopez S, Goux X, Echevarria G, Calusinska M, Morel JL, Benizri E (2019a) Community diversity and potential functions of rhizosphere-associated bacteria of nickel hyperaccumulators found in Albania. *Sci Total Environ* 654:237–249. <https://doi.org/10.1016/j.scitotenv.2018.11.056>
- Lopez S, Goux X, van der Ent A, Erskine PD, Echevarria G, Calusinska M, Morel JL, Benizri E (2019b) Bacterial community diversity in the rhizosphere of nickel hyperaccumulator species of Halmahera Island (Indonesia). *Appl Soil Ecol* 133:70–80. <https://doi.org/10.1016/J.APSOIL.2018.09.007>
- Lopez S, van der Ent A, Sumail S, Sugau JB, Buang MM, Amin Z, Echevarria G, Morel JL, Benizri E (2020) Bacterial community diversity in the rhizosphere of nickel hyperaccumulator plant species from Borneo Island (Malaysia). *Environ Microbiol* 22:1649–1665. <https://doi.org/10.1111/1462-2920.14970>
- Lopez S, Nkrumah PN, Echevarria G, Benizri E, van der Ent A (2021) Bacterial community diversity and functional roles in the rhizosphere of *Rinorea cf. bengalensis* and *Phyllanthus rufuschaneyi* under a nickel concentration gradient. *Plant Soil* 459:343–355. <https://doi.org/10.1007/S11104-020-04763-2/FIGURES/5>
- Lopez S, Morel JL, Benizri E (2022) The parameters determining hyperaccumulator rhizobacteria diversity depend on the study scale. *Sci Total Environ* 834:155274. <https://doi.org/10.1016/J.SCITOTENV.2022.155274>
- Lu LL, Tian SK, Yang XE, Peng HY, Li TQ (2013) Improved cadmium uptake and accumulation in the hyperaccumulator *Sedum alfredii*: The impact of citric acid and tartaric acid. *J Zhejiang Univ Sci B* 14:106–114. <https://doi.org/10.1631/jzus.B1200211>
- Luo LY, Xie LL, Jin DC, Mi BB, Wang DH, Li XF, Dai XZ, Zou XX, Zhang Z, Ma YQ, Liu F (2019) Bacterial community response to cadmium contamination of agricultural paddy soil. *Appl Soil Ecol* 139:100–106. <https://doi.org/10.1016/J.APSOIL.2019.03.022>
- Ma Y, Rajkumar M, Freitas H (2009a) Improvement of plant growth and nickel uptake by nickel resistant-plant-growth promoting bacteria. *J Hazard Mater* 166:1154–1161. <https://doi.org/10.1016/j.jhazmat.2008.12.018>
- Ma Y, Rajkumar M, Freitas H (2009b) Isolation and characterization of Ni mobilizing PGPB from serpentine soils and their potential in promoting plant growth and Ni accumulation by *Brassica* spp. *Chemosphere* 75:719–725. <https://doi.org/10.1016/j.chemosphere.2009.01.056>
- Ma Y, Prasad MNV, Rajkumar M, Freitas H (2011a) Plant growth promoting rhizobacteria and endophytes accelerate phytoremediation of metalliferous soils. *Biotechnol Adv* 29:248–258. <https://doi.org/10.1016/J.BIOTECHADV.2010.12.001>
- Ma Y, Rajkumar M, Luo YM, Freitas H (2011b) Inoculation of endophytic bacteria on host and non-host plants: Effects on plant growth and Ni uptake. *J Hazard Mater* 195:230–237. <https://doi.org/10.1016/j.jhazmat.2011.08.034>
- Ma Y, Rajkumar M, Zhang C, Freitas H (2016) Beneficial role of bacterial endophytes in heavy metal phytoremediation. *J Environ Manage* 174:14–25. <https://doi.org/10.1016/j.jenvman.2016.02.047>
- Martínková L, Uhnáková B, Pátek M, Nešvera J, Křen V (2009) Biodegradation potential of the genus *Rhodococcus*. *Environ Int* 35:162–177. <https://doi.org/10.1016/J.ENVINT.2008.07.018>

- Matchado MS, Lauber M, Reitmeier S, Kacprowski T, Baumbach J, Haller D, List M (2021) Network analysis methods for studying microbial communities: A mini review. *Comput Struct Biotechnol J* 19:2687–2698. <https://doi.org/10.1016/J.CSBJ.2021.05.001>
- Mesa V, Gallego JLR, González-Gil R, Lauga B, Sánchez J, Méndez-García C, Peláez AI (2017) Bacterial, archaeal, and eukaryotic diversity across distinct microhabitats in an acid mine drainage. *Front Microbiol* 8:1756. <https://doi.org/10.3389/FMICB.2017.01756/BIBTEX>
- Myśliwa-Kurdziel B, Prasad MNV, Strzajtka K (2004) Photosynthesis in heavy metal stressed plants. *Heavy Met Stress Plants* 146–181. https://doi.org/10.1007/978-3-662-07743-6_6
- Nkrumah PN, Baker AJM, Chaney RL, Erskine PD, Echevarria G, Morel JL, van der Ent A (2016) Current status and challenges in developing nickel phytomining: An agronomic perspective. *Plant Soil* 406:55–69. <https://doi.org/10.1007/s11104-016-2859-4>
- Parks DH, Chuvochina M, Waite DW, Rinke C, Skarshewski A, Chaumeil PA, Hugenholtz P (2018) A standardized bacterial taxonomy based on genome phylogeny substantially revises the tree of life. *Nat Biotechnol* 36(10):996–1004. <https://doi.org/10.1038/nbt.4229>
- Pillay VK, Nowak J (2011) Inoculum density, temperature, and genotype effects on in vitro growth promotion and epiphytic and endophytic colonization of tomato (*Lycopersicon esculentum* L.) seedlings inoculated with a pseudomonad bacterium. 43:354–361. <https://doi.org/10.1139/M97-049>
- Politi MA, Aparicio JD, Benimeli CS, Amoroso MJ (2014) Role of *Actinobacteria* in bioremediation. *Microb Biodegrad Bioremediation* 269–286. <https://doi.org/10.1016/B978-0-12-800021-2.00011-X>
- Presentato A, Piacenza E, Turner RJ, Zannoni D, Cappelletti M (2020) Processing of metals and metalloids by *Actinobacteria*: Cell resistance mechanisms and synthesis of metal(loid)-based nanostructures. *Microorganisms* 8:2027. <https://doi.org/10.3390/MICROORGANISMS8122027>
- Quast C, Pruesse E, Yilmaz P, Gerken J, Schweer T, Yarza P, Peplies J, Glöckner FO (2013) The SILVA ribosomal RNA gene database project: Improved data processing and web-based tools. *Nucleic Acids Res* 41:590–596. <https://doi.org/10.1093/nar/gks1219>
- R Core Team (2019) R: A Language and Environment for Statistical Computing. R Found Stat Comput Vienna, Austria. <https://www.R-project.org/>
- Rajkumar M, Freitas H (2008) Effects of inoculation of plant-growth promoting bacteria on Ni uptake by Indian mustard. *Bioresour Technol* 99:3491–3498. <https://doi.org/10.1016/j.biortech.2007.07.046>
- Rajkumar M, Sandhya S, Prasad MNV, Freitas H (2012) Perspectives of plant-associated microbes in heavy metal phytoremediation. *Biotechnol Adv* 30:1562–1574. <https://doi.org/10.1016/j.biotechadv.2012.04.011>
- Rastogi G, Osman S, Kukkadapu R, Engelhard M, Vaishampayan PA, Andersen GL, Sani RK (2010) Microbial and mineralogical characterizations of soils collected from the deep biosphere of the former homestake gold mine, South Dakota. *Microb Ecol* 60:539–550. <https://doi.org/10.1007/S00248-010-9657-Y>
- Reeves RD (2003) Tropical hyperaccumulators of metals and their potential for phytoextraction. *Plant Soil* 249:57–65. <https://doi.org/10.1023/A:1022572517197>
- Reinhold-Hurek B, Hurek T (1998) Life in grasses: Diazotrophic endophytes. *Trends Microbiol* 6:139–144. [https://doi.org/10.1016/S0966-842X\(98\)01229-3](https://doi.org/10.1016/S0966-842X(98)01229-3)
- Remenár M, Karellová E, Harichová J, Zámocký M, Krčová K, Ferienc P (2014) *Actinobacteria* occurrence and their metabolic characteristics in the nickel-contaminated soil sample. *Biologia* 69(11):1453–1463. <https://doi.org/10.2478/S11756-014-0451-Z>
- Roane TM, Kellogg ST (1996) Characterization of bacterial communities in heavy metal contaminated soils. *Can J Microbiol* 42:593–603. <https://doi.org/10.1139/M96-080>
- Rosenkranz T, Hipfinger C, Ridard C, Puschenreiter M (2019) A nickel phytomining field trial using *Odontarrhena chalcidica* and *Noccaea goesingensis* on an Austrian serpentine soil. *J Environ Manage* 242:522–528. <https://doi.org/10.1016/J.JENVMAN.2019.04.073>
- Röttgers L, Faust K (2018) From hairballs to hypotheses—biological insights from microbial networks. *FEMS Microbiol Rev* 42:761–780. <https://doi.org/10.1093/FEMSRE/FUY030>
- Saad R, Kobaissi A, Robin C, Echevarria G, Benizri E (2016) Nitrogen fixation and growth of *Lens culinaris* as affected by nickel availability: a pre-requisite for optimization of agromining. *Environ Exp Bot* 131:1–9. <https://doi.org/10.1016/j.envexpbot.2016.06.010>
- Saad RF, Kobaissi A, Echevarria G, Kidd P, Calusinska M, Goux X, Benizri E (2018) Influence of new agromining cropping systems on soil bacterial diversity and the physico-chemical characteristics of an ultramafic soil. *Sci Total Environ* 645:380–392. <https://doi.org/10.1016/j.scitotenv.2018.07.106>
- Sánchez-López AS, Thijs S, Beckers B, Gonzalez-Chavez MC, Weyens N, Carrillo-Gonzalez R, Vangronsveld J (2018) Community structure and diversity of endophytic bacteria in seeds of three consecutive generations of *Crotalaria pumila* growing on metal mine residues. *Plant Soil* 422:51–66. <https://doi.org/10.1007/s11104-017-3176-2>
- Sarkar S, Chakraborty R (2008) Quorum sensing in metal tolerance of *Acinetobacter junii* BB1A is associated with biofilm production. *FEMS Microbiol Lett* 282:160–165. <https://doi.org/10.1111/J.1574-6968.2008.01080.X>
- Sathya A, Vijayabharathi R, Gopalakrishnan S (2017) Plant growth-promoting actinobacteria: a new strategy for enhancing sustainable production and protection of grain legumes. 3 *Biotech* 7:1–10. <https://doi.org/10.1007/S13205-017-0736-3/TABLES/1>
- Schloss PD, Westcott SL, Ryabin T, Hall JR, Hartmann M, Hollister EB, Lesniewski RA, Oakley BB, Parks DH, Robinson CJ, Sahl JW, Stres B, Thallinger GB, Van HDJ, Weber CF (2009) Introducing Mothur: Open-source, platform-independent, community-supported software for describing and comparing microbial communities. *Appl Environ Microbiol* 75:7537–7541. <https://doi.org/10.1128/AEM.01541-09>
- Schnürer J, Rosswall T (1982) Fluorescein diacetate hydrolysis as a measure of total microbial activity in soil and litter. *Appl Environ Microbiol* 43(6):1256–1261. <https://doi.org/10.1128/aem.43.6.1256-1261.1982>
- Seregin IV, Kozhevnikova AD (2006) Physiological role of nickel and its toxic effects on higher plants. *Russ J Plant Physiol* 53:257–277. <https://doi.org/10.1134/S1021443706020178>

- Sessitsch A, Kuffner M, Kidd P, Vangronsveld J, Wenzel WW, Fallmann K, Puschenreiter M (2013) The role of plant-associated bacteria in the mobilization and phytoextraction of trace elements in contaminated soils. *Soil Biol Biochem* 60:182–194. <https://doi.org/10.1016/j.soilbio.2013.01.012>
- Shakya M, Gottle N, Castro H, Yang ZK, Gunter L, Labbé J, Muchero W, Bonito G, Vilgalys R, Tuskan G, Podar M, Schadt CW (2013) A multifactor analysis of fungal and bacterial community structure in the root microbiome of mature *Populus deltoides* trees. *PLoS One* 8:e76382. <https://doi.org/10.1371/journal.pone.0076382>
- Španiel S, Kempa M, Salmerón-Sánchez E, Fuertes-Aguilar J, Mota JF, Al-Shehbaz IA, German DA, Olšavská K, Šingliarová B, Zozomová-Lihová J, Marhold K (2015) AlyBase: database of names, chromosome numbers, and ploidy levels of *Alyssaeae* (Brassicaceae), with a new generic concept of the tribe. *Plant Syst Evol* 301:2463–2491. <https://doi.org/10.1007/s00606-015-1257-3>
- Su J, Ouyang W, Hong Y, Liao D, Khan S, Li H (2016) Responses of endophytic and rhizospheric bacterial communities of salt marsh plant (*Spartina alterniflora*) to polycyclic aromatic hydrocarbons contamination. *J Soils Sediments* 16:707–715. <https://doi.org/10.1007/s11368-015-1217-0>
- Tang X, McBride MB (2018) Phytotoxicity and microbial respiration of Ni-spiked soils after field aging for 12 yr. *Environ Toxicol Chem* 37(7):1933–1939. <https://doi.org/10.1002/etc.4149>
- Tappero R, Peltier E, Gräfe M, Heidel K, Ginder-Vogel M, Livi KJT, Rivers ML, Marcus MA, Chaney RL, Sparks DL (2007) Hyperaccumulator *Alyssum murale* relies on a different metal storage mechanism for cobalt than for nickel. *New Phytol* 175:641–654. <https://doi.org/10.1111/J.1469-8137.2007.02134.X>
- Teitzel GM, Parsek MR (2003) Heavy metal resistance of biofilm and planktonic *Pseudomonas aeruginosa*. *Appl Environ Microbiol* 69:2313–2320. <https://doi.org/10.1128/AEM.69.4.2313-2320.2003/ASSET/11228A19-0EF6-4DB5-8073-888C2D7108D1/ASSETS/GRAPHIC/AM0431749006.JPEG>
- Thompson DK, Wickham G (2018) Gammaproteobacteria and Firmicutes are resistant to long-term chromium exposure in soil. *Adv Microbiol Res* 2:1–6. <https://doi.org/10.24966/AMR-694X/100002>
- Uroz S, Buée M, Murat C, Frey-Klett P, Martin F (2010) Pyrosequencing reveals a contrasted bacterial diversity between oak rhizosphere and surrounding soil. *Environ Microbiol Rep* 2:281–288. <https://doi.org/10.1111/J.1758-2229.2009.00117.X>
- Valls M, De Lorenzo V (2002) Exploiting the genetic and biochemical capacities of bacteria for the remediation of heavy metal pollution. *FEMS Microbiol Rev* 26:327–338. <https://doi.org/10.1111/J.1574-6976.2002.TB00618.X>
- van der Ent A, Baker AJM, Reeves RD, Pollard AJ, Schat H (2013) Hyperaccumulators of metal and metalloids trace elements: Facts and fiction. *Plant Soil* 362:319–334. <https://doi.org/10.1007/s11104-012-1287-3>
- Van der Ent A, Baker AJM, Reeves RD, Chaney RL, Anderson CWN, Meech JA, Erskine PD, Simonnot MO, Vaughan J, Morel JL, Echevarria G, Fogliani B, Rongliang Q, Mulligan DR (2015) Agromining: Farming for metals in the future? *Environ Sci Technol* 49:4773–4780. <https://doi.org/10.1021/es506031u>
- Verbruggen N, Hermans C, Schat H (2009) Molecular mechanisms of metal hyperaccumulation in plants. *New Phytol* 181:759–776. <https://doi.org/10.1111/J.1469-8137.2008.02748.X>
- Visioli G, Vamerali T, Mattarozzi M, Dramis L, Sanangelantoni AM (2015) Combined endophytic inoculants enhance nickel phytoextraction from serpentine soil in the hyperaccumulator *Noccaea caerulea*. *Front Plant Sci* 6:638. <https://doi.org/10.3389/fpls.2015.00638>
- Walker T, Bais H, Grotewold E, Vivanco J (2003) Update on root exudation and rhizosphere biology. *Plant Physiol* 132:44–51
- Xie Y, Fan J, Zhu W, Amombo E, Lou Y, Chen L, Fu J (2016) Effect of heavy metals pollution on soil microbial diversity and bermudagrass genetic variation. *Front Plant Sci* 7:755. <https://doi.org/10.3389/FPLS.2016.00755/BIBTEX>
- Yamada T, Sekiguchi Y (2009) Cultivation of uncultured Chloroflexi subphyla: Significance and ecophysiology of formerly uncultured *Chloroflexi* subphylum I with natural and biotechnological relevance. *Microbes Environ* 71:7493–7503. <https://doi.org/10.1264/jsm2.ME09151S>
- Yamada T, Sekiguchi Y, Imachi H, Kamagata Y, Ohashi A, Harada H (2005) Diversity, localization, and physiological properties of filamentous microbes belonging to *Chloroflexi* subphylum I in mesophilic and thermophilic methanogenic sludge granules. *Appl Environ Microbiol* 71:7493–7503. <https://doi.org/10.1128/AEM.71.11.7493-7503.2005/ASSET/B749209F-AA89-4042-B068-89C48918E2B6/ASSETS/GRAPHIC/ZAM0110559680005.JPEG>
- Zayed A, Gowthaman S, Terry N (1998) Phytoaccumulation of trace elements by Wetland Plants: I. Duckweed. *J Environ Qual* 27:715–721. <https://doi.org/10.2134/JEQ1998.00472425002700030032X>
- Zhuang X, Chen J, Shim H, Bai Z (2007) New advances in plant growth-promoting rhizobacteria for bioremediation. *Environ Int* 33:406–413. <https://doi.org/10.1016/j.envint.2006.12.005>

Publisher's note Springer Nature remains neutral with regard to jurisdictional claims in published maps and institutional affiliations.

Springer Nature or its licensor (e.g. a society or other partner) holds exclusive rights to this article under a publishing agreement with the author(s) or other rightsholder(s); author self-archiving of the accepted manuscript version of this article is solely governed by the terms of such publishing agreement and applicable law.